5.14 The Stable Isotopic Composition of Atmospheric O_2

B Luz and E Barkan, Hebrew University of Jerusalem, Jerusalem, Israel
JP Severinghaus, University of California San Diego, La Jolla, CA, USA

5.14.1 Introduction

During the 1930s, Harold Urey and his collaborators demonstrated that ratios between heavy to light isotopes of the same element varied among various compounds that occur in nature and in the laboratory. They were successful in developing a theory that explained many of the observed variations from differences in the vibrational frequency of molecules (Urey, 1947) and thus obtained convincing evidence that isotopes of the same element differed not only in atomic mass but also in chemical properties. Using this theory, Urey and Greiff (1935) calculated equilibrium constants for exchange reactions involving light elements, such as carbon, oxygen, and sulfur. From the evaluations of the effect of the isotopic exchange, they could predict appreciable variations of atomic weights. Indeed, shortly after the publication of Urey and Greiff's paper, two independent laboratories discovered that the atomic weight of atmospheric oxygen was considerably larger than the atomic weight of oxygen in water (Dole, 1935; Morita, 1935).

For the 30 years that followed this discovery, Dole and his collaborators, almost alone, worked on the global cycle of oxygen and its isotopes. In a review in 1965, Dole concluded that the primary cause for the difference in atomic weight of oxygen between air and water is isotopic fractionation (to be defined in the following section) taking place during respiration by various organisms. The difference in the isotopic composition between atmospheric O_2 and ocean water is named the 'Dole effect' (DE) after Dole who discovered it and devoted many years of his career to studying much about its global controlling mechanisms. Yet, much remained to be discovered and understood about this effect after Dole had left the scene, and an updated review on the DE is given in the succeeding section.

Oxygen has three naturally occurring stable isotopes of atomic mass numbers 16, 17, and 18. The difference between the atomic weights of oxygen in water and air (DE) is caused mainly by differences in the ratio $^{18}O/^{16}O$, and most studies on stable oxygen isotopes deal with variations in the $^{18}O/^{16}O$ ratio. This is so because until 1973 it was thought that all natural processes causing variations in stable isotopic ratios are mass-dependent. In this case, relative variations in the $^{17}O/^{16}O$ ratio are expected to be only about one-half those in the $^{18}O/^{16}O$ ratio. The discovery that in meteorites, variations in $^{17}O/^{16}O$ are about the same as in $^{18}O/^{16}O$ rather than one-half (Clayton et al., 1973) changed that view and showed that mass-independent processes occur in nature. After this discovery, Thiemens and his collaborators started in 1983 a successful line of research and demonstrated that mass-independent fractionations are quite common and important both in the laboratory and in field observations (Thiemens, 1999). Motivated by these studies, Luz et al. (1999) studied atmospheric O_2 and showed that it has a deficit of ^{17}O due to photochemical reactions among O_2, ozone, and CO_2 in the stratosphere. Among other factors, the extent of this deficiency depends on the rate of photosynthesis and is thus useful in studies involving marine and global production of O_2 by plants (e.g., Blunier et al., 2002; Luz and Barkan, 2000, 2009). Variations in both the $^{18}O/^{16}O$ and $^{17}O/^{16}O$ ratio in molecular O_2 and their significance in geochemistry are reviewed in the succeeding dedicated section.

5.14.2 Methodology and Terminology

5.14.2.1 Abundance and Fractionation of Oxygen Isotopes

As defined in classical chemistry, elements that differ only in numbers of neutrons are called *isotopes*. Many elements have two, or more, naturally occurring isotopes. In the case of oxygen, there are three stable (nonradioactive) isotopes ^{16}O, ^{17}O, and ^{18}O. Their nominal abundances are about 99.76, 0.04, and 0.20%, respectively. The superscripts (16, 17, and 18) refer to their atomic masses.

In isotope geochemistry, abundances of rare isotopes are expressed by the ratio of rare/abundant isotope ($^*X$). For example, for H_2O, this ratio is defined as

$$^*X(H_2O) = \frac{(^*O \text{ in water})}{(^{16}O \text{ in water})} \quad [1]$$

where '*' stands for 17 or 18.

The ratios $^*X$ can be measured with very high precision with mass spectrometers (for more details, see Mook, 2000). These isotope ratios are usually not measured on the pure elements, but instead on a gas containing the element under consideration. For most purposes, oxygen isotope ratios are measured on O_2 or CO_2. The common procedure is to compare the isotope ratio of a sample relative to that of a standard, which is assumed to have a known isotopic ratio. In this way, variations due to instrumental drifts and instabilities are considerably reduced because they occur in both sample and standard and cancel out. Using international standards has an additional advantage because it allows comparison of isotopic ratios among laboratories.

Because the measurements are done with respect to standards, it is customary to report the results as deviations (δ) of the isotope ratio of a sample from that of a standard:

$$^*\delta = \frac{^*X_{sample} - {}^*X_{standard}}{^*X_{standard}} = \frac{^*X_{sample}}{^*X_{standard}} - 1 \quad [2]$$

As can be seen, the δ value is dimensionless. For natural substances, the δ values are small, and thus, they are usually multiplied by 10^3 and given in ‰ (per mil).

For a specific isotope (e.g., ^{18}O in O_2), eqn [2] is usually presented in the form

$$\delta^{18}O = \frac{(^{18}O/^{16}O)_{sample}}{(^{18}O/^{16}O)_{standard}} - 1 \quad [3]$$

The choice of standard depends on the material being analyzed. In the case of O_2 gas, measurements are performed directly on the material of interest, and atmospheric O_2 is an ideal standard because atmospheric mixing is very rapid compared to the processes altering the isotopic composition of oxygen and, therefore, $\delta^{18}O$ and $\delta^{17}O$ of atmospheric O_2 are very uniform.

In contrast, in the case of water, most measurements are not done on the original material. Instead, they are performed on gaseous CO_2 or O_2 reacted with or obtained from samples and standards, and the Vienna Standard Mean Ocean Water (VSMOW) standard is used for water. These standards have been discussed in detail in various publications (e.g., Coplen, 1994; Coplen et al., 1983; Gonfiantini, 1978), so here, only a short summary is given.

Standard, VSMOW is a well-preserved batch of distilled water prepared mainly from ocean water. In 1976, it was decided by the International Atomic Energy Agency (IAEA) to use VSMOW for fixing the zero point of the $\delta^{18}O$ water scale ($\delta^{18}O_{VSMOW} \equiv 0$). Analyses of $^{18}O^{16}O$ are performed by equilibrating a water sample with CO_2 of a known isotopic composition, followed by mass spectrometric analysis of equilibrated CO_2. Usually, water samples consisting of unknown samples are run together with the standard or some laboratory reference water well calibrated relative to VSMOW. Samples and standards are run under the same conditions:

$$\delta^{18}O(\text{sample vs. VSMOW}) = \delta^{18}O(\text{sample } CO_2 \text{ vs. VSMOW-}CO_2) \quad [4]$$

The relationship between VSMOW and air O_2 is known from Barkan and Luz (2011) as

$$\delta^{18}O_{gas}(\text{vs. VSMOW}) = 0.97668\delta^{18}O_{gas}(\text{vs. air } O_2) - 23.324$$

Measurements of $\delta^{17}O$ are difficult, first, because ^{17}O is less abundant than ^{18}O by a factor of about five and, second, because precise measurements are not possible with CO_2 gas. The reason for this is the masking effect of the much more abundant ^{13}C on the isotopically substituted CO_2 at the same molecular mass of 45 ($^{13}C^{16}O^{16}O$ and $^{12}C^{17}O^{16}O$). It is noted that even with the recent elegant development of Assonov and Brenninkmeijer (2001), the measurement precision of $\delta^{17}O$ in CO_2 gas was only ±0.3‰. Such precision is insufficient for most geochemical applications.

Measurements of $\delta^{17}O$ are straightforward on pure O_2 gas and with proper correction also in O_2+Ar mixture (Barkan and Luz, 2003). In the case of water, it can be quantitatively converted to O_2 gas by fluorination using CoF_3:

$$2H_2O + 4CoF_3 = 4CoF_2 + 4HF + O_2 \quad [5]$$

Barkan and Luz (2005) applied this method and demonstrated very high precision (0.01–0.03‰) in measurements of both $\delta^{17}O$ and $\delta^{18}O$.

5.14.2.1.1 *Isotopic fractionation*

The chemical and physical properties of compounds containing rare isotopes are very similar to those of the same compound containing major isotopes. Nonetheless, there are small differences in the physical properties (e.g., density, vapor pressure, boiling, and melting points) mainly due to the higher vibration energy of the lighter isotope and higher binding energies in the heavier molecules (Bigeleisen, 1952; Bigeleisen and Wolfsberg, 1958; Urey, 1947). Consequently, as a rule, lighter molecules have higher zero-point energies and react and move faster. This results, for example, in smaller evaporation pressure of $H_2{}^{18}O$ than $H_2{}^{16}O$ and smaller respiration rate of $^{18}O^{16}O$ than $^{16}O^{16}O$.

The above differences lead to separation of isotopic compounds during processes such as evaporation or condensation, melting or crystallization, diffusion in different media, and isotopic exchange reactions in chemical equilibrium (e.g., dissolved CO_2 and bicarbonate) or in physical reactions (e.g., water vapor and liquid water). Such separation is called *isotope fractionation*. The extent of this fractionation depends on mass differences among various isotopes and on

temperature. For example, fractionation is about twice as large for $^{18}O^{16}O/^{16}O^{16}O$ as for $^{17}O^{16}O/^{16}O^{16}O$, or in other words, variations in $\delta^{17}O$ are about one-half those in $\delta^{18}O$.

The isotope fractionation is described mathematically by comparing the isotope ratios of two compounds in equilibrium or of the compounds before and after physical or chemical process (e.g., Mook, 2000). A quantity known as the *fractionation factor* (α) is defined as

$$\alpha_{B/A} = \frac{X_B}{X_A} \quad [6a]$$

or

$$\alpha_{A/B} = \frac{X_A}{X_B} \quad [6b]$$

Equations [6a] and [6b] express the isotope ratio in the phase or compound B relative to that in A or vice versa. For example, X_A may represent $^{18}O/^{16}O$ (or $^{18}O^{16}O/^{16}O^{16}O$) in O_2 reservoir and X_B $^{18}O/^{16}O$ (or $^{18}O^{16}O/^{16}O^{16}O$) in O_2 removed by respiration. In this case, α is known as the *respiratory fractionation factor*.

Typically, fractionation factors are quantities slightly larger [6b] or smaller [6a] than unity (e.g., $\alpha_{B/A} = 0.9800$ and $\alpha_{A/B} = 1.0204$). Often, it is convenient to express fractionation as isotope effect (ε), and the relation between α and ε is

$$\varepsilon = \alpha - 1 \quad [7]$$

Because magnitudes of ε are always small, they are multiplied by 1000 and reported in ‰. For example, $\varepsilon_{B/A}$ for ordinary respiration is about −20‰ (or $\varepsilon_{A/B} = 20.4$‰).

Comparing eqns [6] and [7] clearly shows that while fractionation factors are multiplicative ($\alpha_{total} = \alpha_1\alpha_2 \ldots \alpha_n$), ε is approximately additive ($\varepsilon_{total} \approx \varepsilon_1 + \varepsilon_2 + \ldots + \varepsilon_n$). This explains why in precise calculations of fractionations that result from more than one process, it is necessary to use α and not ε.

Isotope effects can be measured directly in cases where the two phases or compounds are available. For example, the isotope effect of photosynthesis can be measured by comparison of $\delta^{18}O$ of O_2 formed by this process from water to $\delta^{18}O$ of the water substrate. However, for certain processes, such as respiration, it is either impossible or not practical to measure the starting and end materials. In such cases, the isotope effect (ε) is determined from fractionation experiments in which a starting amount of material is lost by a process whose isotope effect is unknown (e.g., evaporation or respiration) and from the change in isotopic ratio X ($^{18}O/^{16}O$ or $^{17}O/^{16}O$) as the amount of the material (N) goes down (such experiments are known as Rayleigh fractionation experiments in the stable isotope literature):

$$\ln\frac{X}{X_0} = \left(\frac{1}{\alpha - 1}\right)\ln\left(\frac{N}{N_0}\right) \quad [8]$$

where the subscript 0 stands for initial X and N (see Mook (2000) for further detail).

An example of the derivation of soil respiratory fractionation from a Rayleigh experiment is shown in Figure 1. Soil was placed in a closed and dark container and the fraction of remaining oxygen and its $\delta^{18}O$ were recorded. The results are shown in Figure 1. In this particular experiment, the consumption of ^{16}O was about 1.5% faster than ^{18}O consumption. Because of this difference in consumption rates, the ratio

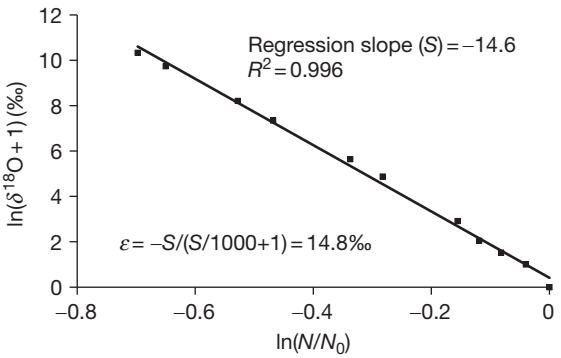

Figure 1 $\ln(\delta^{18}O + 1)$ versus $\ln(N/N_0)$ in Rayleigh fractionation.

$^{18}O/^{16}O$ increased as the remaining fraction of O_2 went down. The isotope effect (ε) was calculated from the regression slope in Figure 1 as 14.8‰.

5.14.2.2 Relationships between Fractionations of $^{17}O/^{16}O$ and $^{18}O/^{16}O$

In certain geochemical studies, such as the isotopic composition of atmospheric O_2, it is of interest to know the relationships between fractionations of $^{17}O/^{16}O$ and $^{18}O/^{16}O$. For most terrestrial processes, this relation is mass-dependent and can be derived from theoretical considerations (e.g., Matsuhisa et al., 1978; Weston, 1999; Young et al., 2002) showing that

$$^{m+1}\alpha_{A/B} = \left(^{m+2}\alpha_{A/B}\right)^{\lambda} \quad \text{or} \quad \ln\left(^{m+1}\alpha_{A/B}\right) = \lambda \ln\left(^{m+2}\alpha_{A/B}\right) \quad [9]$$

where m is the mass of the abundant isotope (16 in the case of oxygen).

For mass-dependent fractionations, the value of factor λ is slightly larger than 0.5. For example, in the case of respiratory fractionation of $^{17}O/^{16}O$ and $^{18}O/^{16}O$, it can be approximated as $0.515 = \ln(16/17)/\ln(16/18)$ (e.g., Young et al., 2002).

Experimental studies showed that indeed in most natural processes the fractionation for the heaviest isotope is about twice as large as that for the lighter isotope (Barkan and Luz, 2007; Helman et al., 2005; Miller et al., 2002). It was also shown that the factor λ varies slightly (0.500−0.529) depending on the isotope fractionation processes (kinetic or steady state) and among the various biological processes. When results of a Rayleigh process (eqn [10]) are displayed in $\ln(\delta^{17}O + 1)$ versus $\ln(\delta^{18}O + 1)$ plots, they fall on straight lines. An example of such a process is given in Figure 2 for the case of O_2 consumption by respiration. As can be seen, the $\ln(^{17}\alpha)/\ln(^{18}\alpha)$ slope (λ) in this experiment equals 0.518, which is nearly as expected from theory.

Whereas mass-dependent fractionation is the rule for most terrestrial processes, there are exceptions with mass-independent fractionation in which λ is much greater than 0.52 (e.g., Clayton et al., 1973; Thiemens and Heidenrich, 1983). For example, the isotopic composition of atmospheric O_2 is affected by photochemical reactions in the stratosphere (e.g., Luz et al., 1999; Thiemens, 1999). Due to these reactions, ozone and CO_2 in the stratosphere have anomalously high $\delta^{17}O$, and atmospheric O_2 is anomalously low in $\delta^{17}O$ in comparison with O_2 produced from water by photosynthesis (Luz et al., 1999).

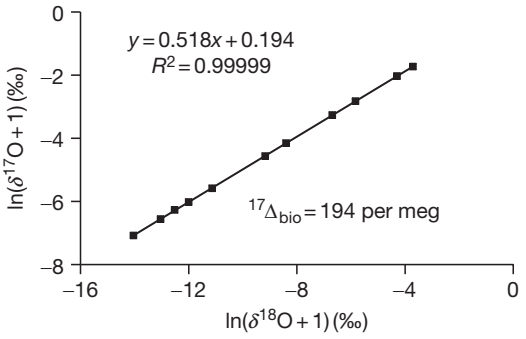

Figure 2 $\ln(\delta^{17}O+1)$ versus $\ln(\delta^{18}O+1)$ in Rayleigh respiratory fractionation.

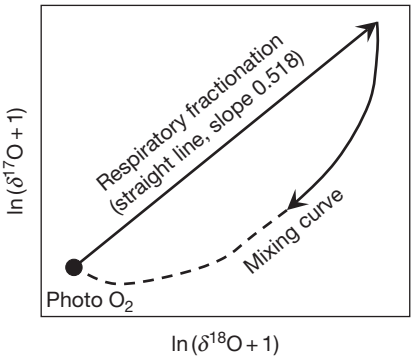

Figure 3 $\ln(\delta^{17}O+1)$ versus $\ln(\delta^{18}O+1)$ showing that respiratory fractionation results in isotopic composition changing along a straight line. Photosynthesis adds new O_2 that mixes with existing O_2 along a curved line.

Deviations from mass-dependent behavior have been described in the literature, and in many cases, the anomaly of ^{17}O ($\Delta^{17}O$) was calculated as $\Delta^{17}O = \delta^{17}O - 0.52\delta^{18}O$ (e.g., Thiemens, 1999). Yet, as discussed by Miller (2002), differences among calculated values of $\Delta^{17}O$ of various materials depend on the choice of isotopic references. To overcome this problem and in order to facilitate direct comparison of results among laboratories, he proposed using natural log transformed deltas (e.g., $\ln(\delta^{17}O+1)$ instead of $\delta^{17}O$). Following Miller (2002), Luz and Barkan (2005) defined a useful parameter ($^{17}\Delta$) for studies of atmospheric and marine dissolved O_2:

$$^{17}\Delta = \ln\left(\delta^{17}O + 1\right) - \lambda \ln\left(\delta^{18}O + 1\right) \qquad [10]$$

The $^{17}\Delta$ parameter indicates an excess or deficit of ^{17}O in a sample with respect to the atmospheric O_2. Because the magnitudes of $^{17}\Delta$ values calculated with eqn [10] are very small, they are multiplied by 10^6 and the reported values are in per meg.

From eqn [10], it is clear that the magnitude of a calculated $^{17}\Delta$ depends on the chosen value of λ and that the absolute value of this magnitude will increase when $\delta^{17}O$ and $\delta^{18}O$ of measured samples are large. Luz and Barkan (2005) discussed such $\delta^{17}O$, $\delta^{18}O$, and $^{17}\Delta$ in studies of dissolved marine O_2. In such studies, it is advantageous to use atmospheric O_2 as a standard (rather than VSMOW) because measured $\delta^{17}O$ and $\delta^{18}O$ values are generally close to those of atmospheric oxygen. In addition, the reference slope λ should be selected such that it optimally fits the system under consideration, and in this respect, a value of 0.518 is optimal for studies of marine dissolved O_2.

It is evident that a Rayleigh process will result in perfectly linear trends in plots of $\ln(\delta^{17}O+1)$ versus $\ln(\delta^{18}O+1)$, and Figure 2 is a good illustration of such linearity. However, when two O_2 volumes having different isotopic composition are mixed, the resulting mixtures will have isotopic compositions that fall on curves in $\ln(\delta^{17}O+1)$ versus $\ln(\delta^{18}O+1)$ plots. Such mixing, for example, takes place when photosynthetic O_2 is added to an existing reservoir of dissolved O_2 (Figure 3).

5.14.3 $^{18}O/^{16}O$ Ratios in Atmospheric O_2

5.14.3.1 The Dole Effect and Its Magnitude

On timescales of thousands of years, the concentration of atmospheric O_2 is held nearly constant by equal rates of photosynthetic production and respiratory consumption (e.g., Broecker, 1970). Because the substrate from which photosynthesis produces O_2 is water, and because the ocean is, by far, the largest reservoir of water on Earth, the $\delta^{18}O$ of atmospheric O_2 must be strongly linked to that of seawater. Nevertheless, as demonstrated independently by Dole (1935) and Morita (1935), the isotopic composition of H_2O and air O_2 is not identical, and the latter is enriched in ^{18}O. The deviation of $\delta^{18}O$ of air O_2 from that of seawater oxygen is known as the DE.

An accurate determination of the value of the DE was first published by Kroopnick and Craig (1972) as $23.5 \pm 0.3‰$. They applied the CO_2 equilibration method for measuring $\delta^{18}O$ of the SMOW standard (which represents seawater), while CO_2 produced by the oxidation of graphite with oxygen gas was used for the measurement of $\delta^{18}O$ of atmospheric O_2. The value determined in this case depends on the fractionation factor for the equilibrium of CO_2 with water. This factor varies in the range 1.0407–1.0417 (e.g., Brenninkmeijer et al., 1983) and is a main source of uncertainty in the DE magnitude. To circumvent this problem, Horibe et al. (1973) converted atmospheric O_2 to water (by oxidation of H_2 gas) and then used the CO_2 equilibration method for measuring $\delta^{18}O$ of this water and also that of the seawater standard SMOW. The magnitude in this case was $23.8 \pm 0.3‰$. By avoiding the problem of CO_2–H_2O equilibration in an alternative way, Barkan and Luz (2005) obtained a value of $23.88 \pm 0.02‰$ by direct comparison of the isotopic composition of atmospheric oxygen with O_2 produced by fluorination of the VSMOW standard.

5.14.3.2 Processes Influencing the Dole Effect

5.14.3.2.1 *Biological O_2 consumption*

The major causes of the DE are biological processes that preferentially consume O_2 molecules containing only light stable isotopes ($^{16}O^{16}O$). The result of this consumption is that O_2 molecules containing heavier isotopes ($^{17}O^{16}O$ and $^{18}O^{16}O$) become enriched in the remaining gas. The magnitude of such fractionations has been studied primarily in small-scale Rayleigh-type experimental systems (see Section 5.14.2.1) and also in large-scale field experiments.

Rabinowitch (1945) was the first to suggest that the cause of the DE might be isotopic fractionation during respiration. Following his suggestion, Lane and Dole (1956) conducted simple respiration experiments and found preferential

consumption of ^{16}O over ^{18}O ($^{18}\varepsilon$) of 7–25‰. Similar simple experiments with natural plankton or cultures of marine organisms were done by Kroopnick (1975), Kiddon et al. (1993), Quay et al. (1995), and Luz et al. (2002). Kiddon et al. (1993) determined the discrimination by main marine eukaryotes as 21‰, but weaker by bacteria (19‰). Kroopnick (1975), in experiments with surface ocean communities, obtained an average respiratory fractionation of 20.8‰, while Luz et al. (2002) reported a value of 21.6‰ for Lake Kinneret in which the plankton community is dominated by phytoplankton. Weaker fractionation (17.6‰) was obtained by Quay et al. (1995) for the Amazon River where O_2 uptake is dominated by bacteria.

In experiments with plants and phytoplankton, Guy et al. (1989, 1992) showed that $^{18}\varepsilon$ in ordinary respiration through the cytochrome oxidase (COX) pathway was 17.4–19.9‰, and much larger $^{18}\varepsilon$ (24.1–26.2‰) was associated with the alternative oxidase (AOX), which is resistant to cyanide. They also pointed out that in large objects, O_2 supply is limited by slow diffusion and suggested that this was the reason for very weak fractionation in intact carrot and potato (8–10‰) in the early experiments of Lane and Dole (1956). In an opposite way, this may also be the reason for the larger $^{18}\varepsilon$ values (~21‰ for COX and ~32‰ for AOX) reported from measurements of isolated mitochondria by Ribas-Carbo et al. (1995). The same authors also showed that $^{18}\varepsilon$ values due to AOX were larger in green tissues than in nongreen tissues (30–32‰ and 24–26‰, respectively).

All the experiments described above were done in darkness in order to avoid interference from O_2 addition by photosynthesis, but, by their design, such dark experiments are not useful for measuring O_2 consumption by mechanisms that are engaged only under illumination. One of these mechanisms is photorespiration, which involves two enzymes, rubisco oxygenase and glycolate oxidase, and is engaged when CO_2 supply is below optimum for plant growth. It is estimated that some 30% of the global photosynthetic production of O_2 is consumed by photorespiration (Bender et al., 1994). Additional O_2-consuming processes that require light are Mehler reaction (Mehler, 1951), chlororespiration (Bennoun, 1994), and the plastoquinol terminal oxidase (Bailey et al., 2008).

Guy et al. (1993) designed special experimental setups for *in vitro* measurement of $^{18}O/^{16}O$ isotope effects ($^{18}\varepsilon$) of Mehler reaction, rubisco oxygenase, and glycolate oxidase in the absence of O_2 production by photosynthesis. Later on, Helman et al. (2005) followed Guy et al.'s (1993) design and ran similar experiments in which they measured, in addition to $^{18}\varepsilon$, the $^{17}O/^{16}O$ isotope effects ($^{17}\varepsilon$). The $^{18}\varepsilon$ results from all these experiments range from about 11‰ for Mehler reaction to 22‰ for glycolate oxidase (see **Table 1** for more details). The magnitude of $^{18}\varepsilon$ associated with O_2 consumption by chlororespiration or the plastoquinol terminal oxidase is unknown.

From the results of the experimental work reviewed earlier, it is clear that biological consumption of O_2 is an important factor in the DE. However, the range of $^{18}\varepsilon$ values in various organisms and biological mechanisms is very broad (11–32‰), and there is no a priori way to accurately obtain a weighted average $^{18}\varepsilon$ of relevance for global calculations of the DE. Fortunately, certain globally important systems lend themselves to large-scale field experiments that are useful for estimating overall biological fractionations relevant for understanding the DE. These systems include soils and the ocean below the surface photic zone.

Excluding light-dependent mechanisms, such as photorespiration and Mehler reaction, soils are the major O_2-consuming systems in the terrestrial environment. Soils contain variable amounts of air in passages among soil particles. Because air diffusion into soils is always limited to a certain extent and because roots and bacteria respire, O_2 concentration in soil air is generally significantly lower than that in the overlaying atmosphere. Likewise, due to respiration, $\delta^{18}O$ of soil air is greater than that of atmospheric O_2. These differences make it possible to calculate effective $^{18}\varepsilon$ ($^{18}\varepsilon_{effective}$) of soil O_2 uptake from measurements of the ratio O_2/Ar and $\delta^{18}O$ in soil air. The effects of slow diffusion on $^{18}\varepsilon_{effective}$ of soils have been studied extensively by Angert and Luz (2001) and Angert et al. (2001, 2003a).

When O_2 is respired in roots or microorganisms in soil aggregates, $^{18}\varepsilon_{effective}$ is influenced by $^{18}\varepsilon$ of respiration ($^{18}\varepsilon_r$) and by $^{18}\varepsilon$ of O_2 diffusion ($^{18}\varepsilon_{diff}$) in air or water. In soils, several steps of diffusion and respiration occur in series, but the resulting effective fractionation cannot be simply calculated by addition of the effects in each of these steps. The total effect of a series of fractionating steps has been treated theoretically by Farquhar et al. (1982). Following them in simple case of O_2 consumption in an airtight chamber by plant roots or soil aggregates (**Figure 4**), $\varepsilon_{effective}$ is expressed by

Table 1 Isotopic effects in biological O_2 uptake processes

	$^{18}\varepsilon$ (‰)	$^{17}\varepsilon/^{18}\varepsilon$
Ordinary respiration by cytochrome oxidase (COX)	17.4–19.9 (Guy et al., 1989, 1992)	0.518 (Angert et al., 2003a; Luz and Barkan, 2005)
Cyanide resistant respiration by alternative oxidase (AOX)	24.1–26.2 (Guy et al., 1989, 1992)	0.518 (Angert et al., 2003a; Luz and Barkan, 2005)
Mehler reaction – reduction of O_2 to produce water when photosynthetic production of O_2 is high	10.9–15.3 (Guy et al., 1993; Helman et al., 2005)	0.526 (Helman et al., 2005)
Photorespiration – O_2 consumption when CO_2 supply is limited		
Occurs in two steps:		
1. By rubisco oxygenase	21.3–21.8 (Guy et al., 1993; Helman et al., 2005)	0.517 (Helman et al., 2005)
2. By glycolate oxidase	22.0–22.7 (Guy et al., 1993; Helman et al., 2005)	0.501 (Helman et al., 2005)

$$^{18}\varepsilon_{\text{effective}} = {}^{18}\varepsilon_{\text{diff}} + \frac{(^{18}\varepsilon_{\text{r}} - {}^{18}\varepsilon_{\text{diff}})[O_2]_i}{[O_2]_a} \quad [11]$$

where $[O_2]_i$ and $[O_2]_a$ stand for O_2 concentration inside the root or aggregate and in the chamber, respectively. For root walls and often for soil aggregates, O_2 diffusion is through water in which $^{18}\varepsilon_{\text{diff}}$ is very small (Farquhar and Lloyd, 1993). Taking it as zero, the equation simplifies to $^{18}\varepsilon_{\text{effective}} = (^{18}\varepsilon_{\text{r}}[O_2]_i)/[O_2]_a$ In turn, the ratio $[O_2]_i/[O_2]_a$ is unity when O_2 is free to move back and forth from the root to the chamber free space and vice versa and becomes smaller when resistance to O_2 exchange becomes stronger. Accordingly, $^{18}\varepsilon_{\text{effective}}$ will equal $^{18}\varepsilon_{\text{r}}$ or become much smaller, respectively. Such simple relationships have been demonstrated in experiments (**Table 2**) that showed that $^{18}\varepsilon_{\text{effective}}$ of soil aggregates decreased by wetting them with water. The added water increased resistance to O_2 exchange and consequently $[O_2]_i/[O_2]_a$ must have been also decreased. As a result, $^{18}\varepsilon_{\text{effective}}$ became smaller. An opposite tendency was demonstrated by disaggregation and suspension of small soil particles in water. There was little resistance to O_2 exchange by these small particles, $[O_2]_i/[O_2]_a$ must have been close to unity, and $^{18}\varepsilon_{\text{effective}}$ increased significantly.

In soils, the situation is more complex. They can be pictured as a mixture of small soil aggregates, roots, and free passages among them. The free space of the passages may be occupied by air, water, or both. Respiration and associated isotope effects take place in roots and aggregates, and in addition, there are also isotope effects of diffusion on a micro scale, and the latter may be quite large (e.g., Aggarwal et al., 2004). Yet, there is no practical way for estimating the isotope effects of each of these processes in individual aggregates or roots. It is possible, on the other hand, to assess the overall effective fractionation of the entire soil complex. In doing so, it is assumed that diffusive fractionation in the larger air-filled passages is 14.3‰ as for binary diffusion of O_2 in air (e.g., Mason and Marrero, 1970).

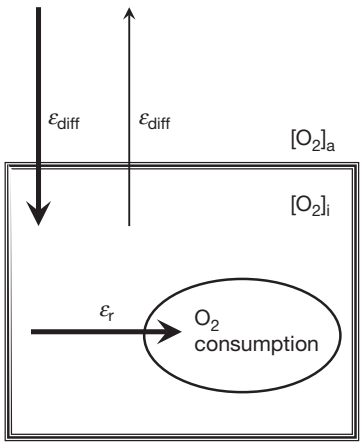

Figure 4 Schematic illustration of effective and respiratory isotope effects.

Table 2 Effects of diffusion on $^{18}\varepsilon_{\text{effective}}$

Incubation experiment	$^{18}\varepsilon_{\text{effective}}$ (‰)
Soil aggregates	13.6
Soil aggregates + water	8.5
Soil disaggregated in water	20.5

Source: Angert A, Luz B, and Yakir D (2001) Fractionation of oxygen isotopes by respiration and diffusion in soils: Implications for the isotopic composition of atmospheric O_2. *Global Biogeochemical Cycles* 14: 871–881.

By applying a model and using measurements of $\delta^{18}O$ and $\delta O_2/Ar$ of soil air, Angert et al. (2003a) estimated $^{18}\varepsilon_{\text{effective}}$ of soils from various climatic regions. These were 10.8, 17.8, and 22.5‰ for tropical, temperate, and boreal soils. From these data, Landais et al. (2007a) calculated a global weighted average of soil fractionation as 15.8‰. The small fractionation in tropical soils may be related to the moisture content blocking free movement of O_2, thus limiting supply to consumption sites. In turn, the larger fractionation in temperate and boreal soils than in tropical soils is likely the result of engagement of respiration through the AOX, which strongly discriminates against ^{18}O. Heat production by AOX is probably advantageous at low soil temperatures.

The ocean below the photic zone (usually below ~150 m) is another system where large-scale fractionations can be studied with relative ease. Variations in the concentration of O_2 below the photic zone are controlled primarily by bacterial consumption and horizontal and vertical mixing. Typically, an O_2 minimum zone exists in mid depth of all oceanic basins where bacterial consumption dominates. This minimum zone was targeted by Dole and coworkers for studying $^{18}\varepsilon_{\text{effective}}$ of the deep sea (Rakestraw et al., 1951) because there they expected to find large concentration and isotopic variations. Indeed, they found good correlation between high $^{18}O/^{16}O$ ratios and low O_2 concentration, and the strong positive correlation led them to the conclusion that there is deep metabolism in the ocean. Assuming that mixing played only a minor role, they used a closed-system Rayleigh calculation to derive a weak isotope effect of only several per mil. Following them, Kroopnick and Craig (1976) measured O_2 concentration and $\delta^{18}O$ in several stations in the world ocean. They applied a more sophisticated model in which vertical diffusive mixing was included in addition to respiration and derived an optimal respiratory isotope effect of 10‰, a weak fractionation similar to that reported by Rakestraw et al. (1951). More recently, similar weak fractionation for the O_2 minimum zone has been reported by Bender (1990) and Levine et al. (2009).

Whereas, due to large concentration and isotopic variations, the O_2 minimum zone seems ideal for studying marine isotope effects, the fractionation there is considerably smaller than in laboratory experiments with marine organisms. This raises the question whether these experiments indicate relevant isotope effects for natural marine systems. One possibility is that most of the respiration in the O_2 minimum takes place inside sinking particles into which gas diffusion is slow with steep exterior–interior O_2 gradients. In this case, similarly to roots and soil aggregates, $^{18}\varepsilon_{\text{effective}}$ would be small. And a further question is whether similar fractionation, regardless of its mechanistic explanation, would apply to overall marine respiration.

It is well known that most of the sinking organic matter produced by photosynthesis in the euphotic zone is oxidized at a relatively shallow depth of the subphotic zone (e.g., Jenkins and Goldman, 1985). Away from the equatorial region, there are significant seasonal variations in O_2 concentration in the

subphotic zone, starting with high concentration after the late winter overturn followed by gradual lowering of O_2 levels in the spring–summer stratified period (Figure 5). Because of the seasonal variations in this zone, estimation of the respiratory fractionation is difficult as it requires careful $\delta^{18}O$ measurements of many samples. So such estimation has been done in only one study in the North Atlantic near Bermuda from $\delta^{18}O$ measurements taken from the same samples shown in Figure 5(a) (Luz and Barkan, 2011). As O_2 decreased between March and September, $\delta^{18}O$ of dissolved O_2 increased. Assuming water at 250 m as a closed system, $^{18}\varepsilon_{effective}$ for the subphotic zone can be calculated as 19.7‰ (Figure 5(b)). This calculation is in good agreement with Levine et al.'s (2009) estimate of 19‰ derived from a wide ocean budget for the mesopelagic zone (excluding the equatorial O_2 minimum zone mentioned earlier). Both estimates are in agreement with isotope effects derived from small-scale experiments with bacteria.

An important question is to what extent the O_2 minimum zone impacts the DE. To answer this question, it is instructive to compare respiration rates there to such rates in the subphotic zone. For instance, the respiration rate in the subtropical Atlantic is about 27 μmol kg^{-1} $year^{-1}$ (Figure 5(a)), and rates in the more fertile parts of the ocean must be greater. In contrast, the rate of respiration in the O_2 minimum is very low, and Levine et al. (2009) estimated only ~2.9 μmol kg^{-1} $year^{-1}$ in the 300–1000 m layer of the equatorial Atlantic where $[O_2]$ is minimal. So the respiration rate in the O_2 minimum zone is two orders of magnitude less than the rate in the subphotic zone and the global effect of the small respiratory fractionation in this zone is negligible. Therefore, an overall $\varepsilon_{effective}$ of 19.4 ± 0.5‰ can be taken as a representative value for in situ respiration in the entire ocean below the photic zone.

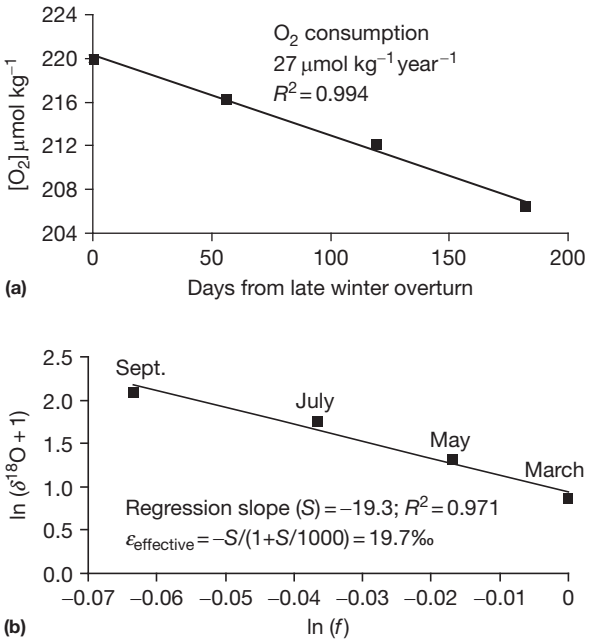

Figure 5 (a) Rate of O_2 consumption in the oceanic thermocline. (b) $^{18}\varepsilon_{effective}$ in the oceanic thermocline.

In summary, the $^{18}\varepsilon_{effective}$ of the dark parts of the ocean of 19.4‰ is larger than that of global soils (~15.8‰). These are the only components of the global O_2 system for which it is possible to derive direct integrated estimates.

In the terrestrial biosphere, aboveground O_2 uptake is probably dominated by photorespiration with combined isotope effects of both rubisco oxygenase and glycolate oxidase of ~21.9‰. O_2 uptake by Mehler reaction ($^{18}\varepsilon$ ~11‰) in leaves is considered to be less than 10% of total O_2 uptake (e.g., Bader et al., 2000), and ordinary and cyanide-resistant respiration is assumed to account for about 16% (Landais et al., 2007a). Some details on the proportions of these O_2 uptake pathways and associated fractionations are given in Table 3. The overall O_2 uptake isotope effect in leaves is ~19.2‰, but there is substantial uncertainty in this value.

In addition to the biological O_2 consumption discussed earlier, it is known that a considerable fraction of the global oxygen uptake takes place in the ocean surface. However, its $^{18}\varepsilon_{effective}$ cannot be estimated without first considering isotopic effects of photosynthesis.

5.14.3.2.2 Photosynthetic O_2 production

With the exception of negligible O_2 production by the photolysis of atmospheric water vapor, all O_2 on Earth is produced by photosynthesis. Knowing this, Dole and Jenks (1944) ran photosynthesis experiments and obtained O_2 gas produced by plants and algae and compared its $^{18}O/^{16}O$ ratio to that of the substrate water. Expressed in the present conventional $\delta^{18}O$ terms, the O_2 gas was enriched in ^{18}O by about 5‰ with respect to the substrate water. However, the validity of this pioneering observation has been repeatedly challenged by several studies (Guy et al., 1993; Helman et al., 2005; Luz and Barkan, 2005; Vinogradov et al., 1959; Yakir et al., 1994). In particular, Guy et al. (1993) demonstrated similar $\delta^{18}O$ of water and photosynthetic O_2 produced by spinach thylakoids, cyanobacteria, and diatoms. Helman et al. (2005) confirmed this observation in experiments with cyanobacteria. Moreover, from mass balance calculations, Luz and Barkan (2005) confirmed the similarity of $\delta^{18}O$ of water and O_2 produced by *Phylodendron*. All these studies led to the understanding that the enrichment reported by Dole and Jenks (1944) does not represent the original isotopic composition of photosynthetic O_2 and was caused by their failure to eliminate partial consumption by respiration and/or atmospheric contamination in their experimental setup.

Table 3 Calculated $^{18}\varepsilon_{effective}$ of O_2 uptake in leaves

Process and fraction of terrestrial gross O_2 production	*$^{18}\varepsilon_{effective}$ (‰)*
Photorespiration (30%)	21.9 ± 1.0
Mehler reaction (10%)	10.9 ± 0.2
COX and AOX respiration (16%)	19.4 ± 1.0
Total leaf O_2 uptake (56%)	19.2 ± 2.0

Source: Landais A, Lathiere J, Barkan E, and Luz B (2007a) Reconsidering the change in global biosphere productivity between the Last Glacial Maximum and present day from the triple oxygen isotopic composition of air trapped in ice cores. *Global Biogeochemical Cycles* 21: GB1025, http://dx.doi.org/10.1029/2006GB002739.

The notion that there is no fractionation of oxygen isotopes during photosynthesis has been deeply entrenched and has guided the interpretation of experimental results until very recently. Yet, failure of global budgets, such as in Bender et al. (1994), to account for the magnitude of the DE has led Eisenstadt et al. (2010) to revisit the problem of possible fractionation in photosynthesis, and they ran photosynthetic experiments in which O_2 was produced by various cultures of marine phytoplankton. These experiments complement a small number of well-controlled ones done by Guy et al. (1993), Luz and Barkan (2005), and Helman et al. (2005).

To yield meaningful results, it is necessary to completely eliminate any respiratory consumption of the newly produced O_2 or alternatively to correct for respiratory consumption. The latter is possible only if accurate rates of gross O_2 production, respiratory consumption, and its isotope effect are known. Accordingly, three experimental setups have been designed:

1. O_2 was produced *in vitro* by thylakoids (photosynthetic membranes) separated from fresh market spinach. These membranes do not respire, and O_2 produced by photosynthesis had $\delta^{18}O$ identical ($\pm 0.2‰$) to that of the substrate water (see Guy et al. (1993) for details).
2. An airtight terrarium experiment was set up under controlled conditions in which $\delta^{18}O$ leaf water was known, photorespiration was prevented by high CO_2 in the terrarium air, and practically all O_2 uptake was by soil respiration, whose $^{18}\varepsilon_{\text{effective}}$ was known from dark experiments. Rates of gross (G) and net (N) O_2 production and thus light O_2 uptake ($U = G - N$) were also known from a separate experiment with the same terrarium using ^{18}O-spiked O_2 gas. More details on the experiment are given in Luz and Barkan (2005). Using their data, it is estimated that ^{18}O of the photosynthetic O_2 was only slightly enriched ($\sim 0.7‰$) with respect to the leaf water.
3. Experiments for O_2 production by marine cyanobacteria and algae have been set up by Guy et al. (1993), Helman et al. (2005), and Eisenstadt et al. (2010). Special attention was paid to prevent $\delta^{18}O$ alteration by partial O_2 consumption or by atmospheric contamination. In order to allow optimal growth conditions and prevent photorespiration, cultured algal and cyanobacteria cells were suspended in an adequate growth medium supplemented with at least 5 mM $NaHCO_3$ and a buffer for maintaining a pH of 8.2 to prevent photorespiration. The light intensity was adjusted for maximal O_2 production. The medium was illuminated and O_2 produced was immediately removed by stirring and vigorously bubbling with 99.999% grade He. Results from these experiments are given in Table 4 and show negligible ($\sim 0.4‰$) to substantial ($\sim 6‰$) ^{18}O enrichment in the newly produced O_2 with respect to the substrate water.

Table 4 Photosynthetic enrichment in ^{18}O in marine phytoplankton

	$\delta^{18}O$ *versus substrate water (‰)*
Cyanobacteria (Helman et al., 2005)	0.47
Green algae (Eisenstadt et al., 2010)	2.85
Diatoms (Eisenstadt et al., 2010)	4.43
Coccolithophores (Eisenstadt et al., 2010)	5.81

Experiments of types 1 and 2 are the only ones giving information relevant to higher plants and thus to terrestrial O_2 production. The results show that O_2 originating from terrestrial photosynthesis is similar or slightly enriched in ^{18}O with respect to leaf water. Experiments of type 3 are relevant to O_2 produced by marine photosynthesis and show that with the exception of cyanobacteria, O_2 originating from marine photosynthesis is enriched in ^{18}O with respect to seawater. The extent of this enrichment in the ocean depends on the proportion of gross production rates by various phytoplankton groups (but not necessarily their abundances). So the overall ^{18}O enrichment in marine systems cannot be easily assessed from a priori consideration. Despite that, ocean-wide estimates of a combined isotope effect due to photosynthesis and O_2 uptake ($^{18}\varepsilon_{\text{up}}$) in the surface ocean can be obtained.

The combined isotope effect in the surface ocean can be determined from the mass balance of ^{18}O in dissolved O_2. Such mass balance should take into account O_2 gains and losses due to photosynthesis, uptake, air–sea gas exchange, and mixing of O_2 from the deeper layer below the surface mixed layer. In a complete mass balance, it is necessary to take account of the temporal changes in the depth of the mixed layer and variations in O_2 concentration and $\delta^{18}O$. A simplified mass balance is possible, if quasi-steady state is assumed in the mixed layer. **Figure 6** shows the major fluxes used in a simple steady-state calculation, neglecting O_2 exchange across the oceanic pycnocline. For such a simplified case, the following mass balance equation can be written (see derivation details in Luz and Barkan, 2011):

$$^{18}\varepsilon_{\text{up}} = \frac{\left[(C/C_{\text{eq}} - 1)R_{\text{w}} + N/G\left(R_{\text{eq}} - C/C_{\text{eq}}R_{\text{dis}}\right)\right]}{\left[(C/C_{\text{eq}} - 1)(1 - N/G)R_{\text{dis}}\right]} - 1 \quad [12]$$

where N is the net O_2 production, G is the gross O_2 production, U is the O_2 uptake by various respiratory mechanisms, C and C_{eq} are measured and equilibrium O_2 concentrations, respectively, and R_{w}, R_{eq}, and R_{dis} stand for $^{18}O^{16}O/^{16}O^{16}O$ ratios in O_2 derived from complete conversion of water to O_2 gas, in O_2 at equilibrium with the atmosphere, and in O_2 dissolved in the ocean, respectively.

Such a calculation was first applied by Quay et al. (1993) who derived $^{18}\varepsilon_{\text{up}}$ of $22 \pm 6‰$ for the subarctic Pacific. The relatively large error in their result was due to uncertainties in the magnitudes of the various fluxes. For a case of much larger biological fluxes (G and N) and small gas exchange in Lake Kinneret, the errors were smaller and Luz et al. (2002) reported $^{18}\varepsilon_{\text{up}}$ ranging 22–25‰. Assuming that there was no fractionation in photosynthesis, they concluded that the larger estimates may be the result of engagement of the AOX pathway which is known to strongly discriminate against ^{18}O (see **Section 5.14.3.2.1**).

Hendricks et al. (2004) proposed a method based on similar fluxes as in eqn [12], but with smaller uncertainties, by using measured $\delta O_2/Ar$, $\delta^{17}O$, and $\delta^{18}O$ of dissolved O_2. In this method, G is estimated from $\delta^{17}O$ and $\delta^{18}O$ (see **Section 5.14.4.1**) and N from $\delta O_2/Ar$. Hendricks et al. (2004, 2005) applied this method in their studies of the Southern Ocean and the equatorial Pacific and estimated the combined respiratory

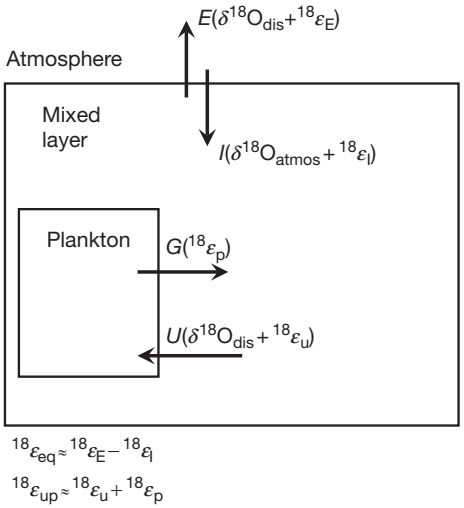

Figure 6 Schematic illustration of O_2 isotope effects in the oceanic mixed layer. ${}^{18}\varepsilon_{eq}$ is the $\delta^{18}O$ difference of dissolved O_2 from atmospheric O_2 due to small equilibrium isotope effect (${}^{18}\varepsilon_I$) in O_2 dissolution. ${}^{18}\varepsilon_{eq}$ is a combined isotope effect that includes ${}^{18}O$ enrichment in photosynthetic production from water (${}^{18}\varepsilon_p$) and further enrichment due to respiratory uptake (${}^{18}\varepsilon_u$).

photosynthesis isotope effect as 22 ± 1 and 21 ± 2‰, respectively. In the same way, Luz and Barkan (2011) applied the method in various marine locations, including two which were sampled during spring blooms. In addition, they applied the method to the largest available database on oceanic $\delta O_2/Ar$, $\delta^{17}O$ and $\delta^{18}O$ (Reuer et al., 2007). Recently, Prokopenko et al. (2011) suggested an improved equation for calculating N/G. Using their equation, ${}^{18}\varepsilon_{up}$ values were recalculated for various ocean locales (Table 5).

From Table 5, it is clear that the magnitudes of ${}^{18}\varepsilon_{up}$ are not randomly distributed in the ocean. Stronger fractionations were observed in oceanic sites which were at their spring blooms or just about to start blooming (S. Ocean and Celtic Sea). However, there is no correspondence between photosynthetic accumulation of O_2, as indicated by $\delta O_2/Ar$ in the Celtic Sea, and ${}^{18}\varepsilon_{up}$. Likewise, there is no correspondence between iron addition and ${}^{18}\varepsilon_{up}$ in the Eisenex experiment in the Southern Ocean. This suggests that before the start of the bloom, the phytoplankton communities were already primed for strong fractionation during O_2 uptake or photosynthesis.

The database of Reuer et al. (2007) that was used for deriving the ${}^{18}\varepsilon_{up}$ for the Southern Ocean is by far the most extensive one available for the world ocean and thus deserves special attention. In Figure 7, all the individual calculated ${}^{18}\varepsilon_{up}$ values were plotted. As can be seen, there is a slight tendency for larger ${}^{18}\varepsilon_{up}$ with increasing net O_2 production. This, in turn, is consistent with the observation of strong fractionation during blooms (Table 5). Because of the broad area covered by this database, the average ${}^{18}\varepsilon_{up}$ of 25.2 ± 1.9‰ can be taken as a representative of the entire ocean. If ${}^{18}\varepsilon_u$ of 19.7‰ for average marine respiration below the photic zone applies also to respiration in the surface ocean, then it can be calculated that ${}^{18}\varepsilon_p=\sim5$‰ for mean oceanic photosynthetic enrichment with respect to seawater.

Table 5 Isotopic effects in the mixed layer

	ε_{up} (‰)
Southern Ocean average[a]	25.2 ± 1.9
Eisenex experiment[b]	
with Fe addition	26.9 ± 0.3
without Fe addition	27.1 ± 0.9
Celtic Sea[b]	
bloom	26.7 ± 1.3
prebloom	25.3 ± 0.6
N. Atlantic near Bermuda[b]	23.7 ± 1.8
Red Sea near Eilat[b]	21.9 ± 1.0

[a]Data from Reuer et al. (2007)
[b]Data from Luz and Barkan, 2011; due to large computation errors, data points for which ${}^{17}\Delta$ and/or N/G were less than 20 per meg and 0.01, respectively, were not used in the calculation of ε_{up}.

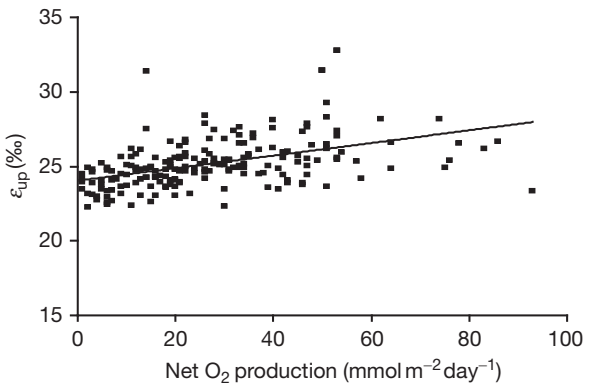

Figure 7 Combined isotopic effect of respiration and photosynthesis in the surface ocean.

5.14.3.2.3 Hydrologic processes

The substrate of O_2 produced by terrestrial photosynthesis is leaf water and therefore its $\delta^{18}O$ is an essential factor of the DE. In turn, $\delta^{18}O$ of leaf water is controlled by two main mechanisms. The first one involves processes that determine $\delta^{18}O$ of meteoric water, and the second involves processes affecting $\delta^{18}O$ of leaf water in plant transpiration.

Isotopic variations in meteoric water have been a target for much investigation starting from the very early days of stable isotope geochemistry. In general, meteoric waters have $\delta^{18}O$ close to that of seawater and become depleted at higher latitudes or high topographic elevations (e.g., Bowen and Revenaugh, 2003; Dansgaard, 1964). Accordingly, water used by plants and trees has a wide range of $\delta^{18}O$ values. These, in turn, increase by leaf transpiration into dry air. The effect of air humidity on $\delta^{18}O$ of leaf water was first studied by Gonfiantini et al. (1965). The cause of the ${}^{18}O$ enrichment in leaf water is similar to that of evaporation from small water bodies. It depends on the liquid–water isotopic equilibrium and on fractionation during the diffusion of water vapor in air. The effect of the latter becomes stronger as air relative humidity goes low (e.g., Gat, 1996). Dongmann et al. (1972) explained that because leaf water is the substrate for terrestrial photosynthetic O_2, the transpiration enrichment mechanism enhances the

magnitude of the DE. Subsequently, Dongmann (1974) estimated the contribution of land photosynthesis to the DE as 8‰. This estimate, however, has been subject to much debate in subsequent publications.

While the general trends of $\delta^{18}O$ in meteoric water and the effects of transpiration on $\delta^{18}O$ of leaf water are well established, the detailed distribution of leaf water and its integrated effect on $\delta^{18}O$ of atmospheric O_2 are very complex. Yet, for the explanation of the isotopic composition of atmospheric O_2, it is the integrated effect of leaf water that is of much importance. An ingenious way for obtaining such an integrated estimate was proposed by Farquhar et al. (1993) from analyses of $\delta^{18}O$ of atmospheric CO_2. It is known that O_2 gas and oxygen in water vapor do not exchange isotopes. In turn, two main reservoirs of water influence $\delta^{18}O$ of atmospheric CO_2 by isotopic exchange, seawater and leaf water. Despite its very small size in comparison to the ocean, leaf water has a major effect. This is because CO_2–H_2O equilibration, through which the isotopic exchange occurs, is very rapid in leaves.

Since the pioneering study of Mills and Urey (1940), it has been known that oxygen isotope exchange takes place between CO_2 and H_2O through the formation of carbonic acid H_2CO_3. However, the reaction of carbon dioxide hydration and dehydration is not instantaneous, and the time for oxygen isotope equilibration between CO_2 and liquid H_2O is on the order of minutes or longer. On the other hand, Roughton (1935) showed that hydration–dehydration is very rapid when it is catalyzed by the enzyme carbonic anhydrase (CA). CA is ubiquitous in leaves and can potentially bring about equilibrium between H_2O and CO_2 during the short transit time of carbon dioxide in photosynthesizing leaves. Indeed, Francey and Tans (1987) found a clear signature of leaf water $\delta^{18}O$ in atmospheric CO_2. Until their study, it was generally believed that the isotopic composition of atmospheric carbon dioxide was dominated by isotopic exchange with the ocean because $\delta^{18}O$ of CO_2 was close to the equilibrium value with seawater (Bottinga and Craig, 1969; Keeling, 1961). However, the observations of Francey and Tans (1987) showed that this could not be the case because $\delta^{18}O$ of CO_2 in high northern latitudes was too low to be explained by equilibration with cold oceanic water. They suggested that their observations were the result of rapid exchange with leaf water.

Farquhar et al. (1993) took the atmospheric observations a step further and constructed a model which included atmospheric mixing times and isotopic exchange between seawater, soil moisture, and leaf water with atmospheric CO_2. A key element in this model is the very rapid CA-catalyzed exchange in leaves in comparison to slow exchange with seawater and soil moisture. Because the isotopic exchange with leaves takes place during photosynthesis inside chloroplasts, $\delta^{18}O$ of chloroplast water affects both atmospheric CO_2 and newly produced O_2. From model calculations, they estimated that 4.4‰ of Earth's DE would result from ^{18}O enrichment of leaf water. This estimate fell several per mil short of the 8‰ that was needed to account for the DE in the global budgets of Dongmann (1974) and Bender et al. (1994).

An explanation for the discrepancy was suggested by Gillon and Yakir (2001), who conducted a survey of CA activity and CO_2 hydration–dehydration rates in species representing trees, shrubs, herbs, and grasses. From these measurements, they calculated the degree of isotopic equilibration for the various plant groups and found that it was low for C_4 grasses. Overall, they reported that global CO_2–H_2O equilibration was not complete and estimated an average equilibration value of ~80%. From this estimate, they suggested that ^{18}O enrichment in leaf water must be larger than in Farquhar et al.'s (1993) calculation and further suggested that ^{18}O enrichment in leaf water accounts for 6–8‰ of the DE.

An alternative way for obtaining a global average of ^{18}O enrichment in leaf water is from direct observations on their $\delta^{18}O$ values. Yet, because of the high variability on $\delta^{18}O$ of leaf water on both temporal and geographical scales, obtaining such a global average is difficult and there is considerable uncertainty in the obtained value. Nevertheless, such averages have been derived and a recent one, based on global models, of 6.5‰ has been published by West et al. (2008). Considering the uncertainty in this estimate (±2.1‰), it is similar to the $\delta^{18}O$ of leaf water suggested by Gillon and Yakir (2001).

5.14.3.2.4 Stratospheric photochemical reactions

Exchange of oxygen isotopes between atmospheric O_2 and CO_2 was suggested by Vinogradov et al. (1959) as a major mechanism for the explanation of the DE. Their argument started from a well-known fact that due to isotopic equilibration between CO_2 and H_2O, atmospheric CO_2 is enriched in ^{18}O by more than 40‰ with respect to seawater. They further suggested that in the stratosphere, UV radiation should cause some transfer of this ^{18}O enriched oxygen from CO_2 to O_2. Yet, they did not have any data to support their hypothesis.

Because of temperature stratification, stratospheric air does not readily exchange with the troposphere and it resides for several years above the tropopause (Appenzeller et al., 1996; Holton, 1990). Therefore, if Vinogradov et al. (1959) were right, stratospheric CO_2 would have been depleted in ^{18}O with respect to that gas in the troposphere. But, in fact, observations show that stratospheric CO_2 is highly enriched in ^{18}O (e.g., Gamo et al., 1989; Lammerzahl et al., 2002). Thus, the Vinogradov et al. (1959) explanation must be ruled out. However, the high ^{18}O enrichment of stratospheric CO_2 is interesting in its own right and will be discussed in **Section 5.14.4.1**. In short, it is caused by mass-independent transfer of ^{18}O and ^{17}O from O_2 to O_3 and then to CO_2 (e.g., Thiemens, 1999).

Because the ultimate source of the heavy oxygen isotopes in stratospheric CO_2 is atmospheric O_2, it is expected that as CO_2 gets enriched, O_2 would become depleted in ^{17}O and ^{18}O. From stratospheric mass balance of oxygen isotopes, Bender et al. (1994) calculated a decrease of about 0.4‰ in both $\delta^{18}O$ and $\delta^{17}O$ of atmospheric O_2. Later on, this mass-independent depletion was experimentally confirmed by Luz et al. (1999), and from their data, about 0.3‰ lowering of $\delta^{18}O$ of atmospheric O_2 by stratospheric photochemistry was estimated. Clearly, the effect of stratospheric photochemistry on atmospheric $\delta^{18}O$ is negligible in comparison to the effect of respiration, photosynthesis, or hydrology. It is noted, however, that, as discussed in **Section 5.14.4.1**, this small mass-independent change in air O_2 can be used for estimating the ratio of gross to net O_2 production in the surface ocean. This ratio, in turn, is very useful for estimating oxygen isotope

effects of respiration and photosynthesis in the ocean (see Section 5.14.3.2.2).

5.14.3.3 Global Budgets of Processes Influencing the Dole Effect

Efforts to explain the DE started after its discovery in 1935 and experiments were set up to find out whether it could result from ^{18}O enrichment in photosynthesis. The first results (Dole and Jenks, 1944) showed some 5‰ enrichment in photosynthetic O_2 with respect to the substrate water. These experiments were followed by the respiration experiments of Lane and Dole (1956) that showed substantial discrimination against ^{18}O in O_2 consumed by respiration and ^{18}O enrichment in the remaining O_2. Dole (1965) reviewed the available information and concluded that, similarly to the elemental O_2 cycle, there was a natural cycle of oxygen isotopes. In his view, when both cycles operated in steady state between production and consumption, atmospheric O_2 became somewhat enriched in ^{18}O in the photosynthetic production step and further enrichment ($\sim$16–18‰) was attributed to respiratory consumption. Given that at the time Dole wrote his review there were no accurate data on the magnitude of the DE, these two enrichments combined seemed sufficient for explaining the measured effect. However, as discussed in Section 5.14.3.2.2, other researchers of his time rejected the idea that O_2 produced by photosynthesis was enriched in ^{18}O with respect to the water substrate. This left the origin of the DE unexplained.

A solution was proposed by Dongmann and his colleagues (Dongmann, 1974; Dongmann et al., 1972) who suggested that the gap could be closed by terrestrial photosynthesis, the substrate of which is leaf water. Based on their measurements, Dongmann and coworkers proposed substantial 8‰ ^{18}O enrichment in leaf water, sufficient for closing the gap.

The idea of Dongmann was further developed by Bender et al. (1994) in a more quantitative way. Bender's group utilized additional information on the biogeochemical mechanisms involved in the global oxygen cycle, as well as more precise experimental data on oxygen isotopic fractionation in various processes. They divided the global DE (DE_{glob}) into two main components: (1) terrestrial DE (DE_{terr}), which is defined as the effect that would result from O_2 exchange by photosynthesis and respiration on land alone, and (2) marine DE (DE_{mar}), which is defined analogously and represents the ocean alone. Following this concept, DE_{glob} is expressed as

$$DE_{glob} = DE_{mar} \times f_{mar} + DE_{terr} \times f_{terr} - \varepsilon_{strat} \qquad [13]$$

where f_{mar} and f_{terr} stand for the fractions of marine and terrestrial gross O_2 production, respectively, and ε_{strat} represents lowering of $\delta^{18}O$ of atmospheric O_2 by stratospheric photochemistry. The values of DE_{terr} and DE_{mar} were estimated as 22.4 and 18.9‰, respectively, and then, taking f_{mar} and f_{terr} as 0.37 and 0.63, respectively, the global DE was calculated as 20.8‰.

By means of the same logic, but with a 3D numerical model, Hoffmann et al. (2004) obtained the following: $DE_{terr}=25.9$‰, $DE_{mar}=17.0$‰, and $DE_{glob}=22.9$‰. The greater DE_{terr} was due to their use of stronger ^{18}O enrichment in leaf water ($\sim$6 instead of 4.4‰). The smaller DE_{mar} was the result of the larger fraction of marine respiration assigned to O_2 uptake at intermediate oceanic depths (0.2 instead of 0.05 in Bender et al., 1994), where the overall fractionation is known to be weaker (Bender, 1990; Kroopnick and Craig, 1976; Levine et al., 2009; Rakestraw et al., 1951). In both cases, the calculated magnitude of DE_{glob} strongly depended on the sizes of f_{mar} and f_{terr}. From this dependence, it was expected that variations in the f_{mar}/f_{terr} ratio would result in changing magnitudes of DE_{glob}.

In the preceding sections, the current understanding of the magnitude of $^{18}O/^{16}O$ fractionation of the major mechanisms that control DE_{glob} has been reviewed. Among these, there are two main observations that were not available to either Bender et al. (1994) or Hoffmann et al. (2004). These are significant fractionation in marine photosynthesis and attenuated fractionation in soil respiration. In the succeeding text, these are included in calculations of DE_{mar} and DE_{terr}.

Following Bender et al. (1994), the marine DE can be expressed as

$$DE_{mar} = f_{surface}DE_{surface} + f_{deep}DE_{deep} \qquad [14]$$

where $f_{surface}$ and f_{deep} are the fractions of O_2 uptake in the surface and deep ocean, respectively. $DE_{surface}$ is the difference between $\delta^{18}O$ of seawater and atmospheric O_2 that would result in a hypothetical case in which the only components are the surface ocean and the atmosphere. DE_{deep} is defined similarly for a case where the deep ocean and the atmosphere are the only components.

$DE_{surface}$ is simply calculated by subtraction of the isotopic effect of the equilibrium isotopic fractionation of dissolved O_2 with respect to atmospheric O_2 ($^{18}\varepsilon_{eq}\approx 0.75$‰) from $^{18}\varepsilon_{up}$ (25.2 ± 1.9‰) as 24.4‰. On the other hand, the in situ fractionation in the deep isolated parts of the ocean (ε_u) is not fully expressed in the atmosphere, but DE_{deep} can be calculated from eqn [15] as (see derivation in Luz and Barkan, 2011)

$$DE_{deep} = \frac{10^3\left[10^{-3}\varepsilon_p(1-f) + f^{\alpha}\left(1+10^{-3}\varepsilon_{eq}\right) - f - 10^{-3}\varepsilon_{eq}\right]}{\left[1-f^{\alpha}\right]} \qquad [15]$$

where $\alpha = 1/(10^{-3}\varepsilon_u + 1)$ and f is the fraction of initial O_2 that remains after respiration took place in an isolated parcel of water in the deep sea. The rest of the parameters are as defined earlier.

From the ratio of respiration to the size of O_2 inventories in the water column just below the illuminated upper ocean where most marine respiration takes place, f can be estimated. At steady state, respiration is equal to the flux of organic aggregates produced in the photic zone, which, in turn, equals net production. Net production was estimated from $\delta O_2/Ar$ and wind speed measurements (e.g., Hendricks et al., 2004) from the vast Southern Ocean database of Reuer et al. (2007) as about 2.7 mol m^{-2}. This amounts to $\sim$6% of the O_2 inventory in the 100–300 m interval ($\sim$44 mol m^{-2}). A similar calculation based on data from the BATS station near Bermuda (Luz and Barkan, 2009) yields $\sim$9%. Thus, f can be taken as 0.91–0.94. Then, substituting $\varepsilon_p = 5$‰, $\alpha = 1/(19.7\times10^{-3}+1)$, and $\varepsilon_{eq}=0.75$‰ into eqn [15], DE_{deep} is obtained as 23.1–23.4‰.

In order to calculate DE_{mar}, the ratio of respiration below the photic zone to respiration in the photic zone needs to be known. Bender et al. (1994) assumed the fraction consumed

below the photic zone as 5% of the total, but they did not argue their choice. In principle, the given ratio corresponds to the N/G ratio, because on several years scale total marine respiration equals gross production (G) and the deep respiration rate equals net production (N). As discussed in Luz and Barkan (2009), correct N/G values should be determined from in situ measurements of O_2/Ar ratio, $^{17}O/^{16}O$, and $^{18}O/^{16}O$ of dissolved O_2 (see Section 5.14.3.2.2). Such N/G estimates were obtained for the subtropical Pacific (average of 0.1; Juranek and Quay, 2005), equatorial Pacific (average of 0.06; Hendricks et al., 2005), Southern Ocean (average of 0.13; Reuer et al., 2007), and the Atlantic Ocean near Bermuda (average of 0.14; Luz and Barkan, 2009). From these ratios, a representative value for N/G ratio in the ocean is estimated as 0.11. So based on ocean-wide information, the fraction of respiration in the deep sea is about 11%.

Finally, using the estimates of $DE_{surface}$, DE_{deep} and the fraction of respiration in the deep sea, DE_{mar} is calculated as 23.3‰ (Table 6). Obviously, there is considerable uncertainty in this value, and its main source is the scatter of $DE_{surface}$ in the database (±1.9‰).

The terrestrial DE can be expressed as

$$DE_{terr} = \delta^{18}O_{leaf\text{-}water} + \varepsilon_{u\text{-}leaves+soil} - \varepsilon_{eq} \qquad [16]$$

As discussed in Section 5.14.3.2.3, the global weighted average of $\delta^{18}O$ of leaf water is 6.5‰. From Section 5.14.3.2.1, the isotopic effects in leaf O_2 uptake and in soil respiration are 19.2 and 15.8‰, respectively, and the weighted average of the overall terrestrial respiratory fractionation ($\varepsilon_{u\text{-}leaves+soil}$) is 17.7‰. Substituting these values in eqn [16] and subtracting 0.75‰ to account for solubility equilibration between air O_2 and oxygen dissolved in leaf water, DE_{terr} can be estimated as 23.5 ± 2.3‰ (Table 6).

By using eqn [16] with values of DE_{mar}, DE_{terr}, ε_{strat}, f_{mar}, and f_{terr} from Table 6, a global estimate of the DE can be calculated as 23.5 ± 2.5‰. Given the calculation uncertainty, this value is equal to the measured DE (23.88‰) and also equal to both calculations of DE_{mar} (24.3 ± 1.1‰) and DE_{terr} (23.5 ± 2.3‰). Clearly, despite uncertainties in the sizes of the fractions of terrestrial and marine productivities in Table 6, the calculated DE_{glob} is not sensitive to the ratio of f_{mar} to f_{terr}. Therefore, variations in f_{mar}/f_{terr} cannot explain the record of past variations in the DE, and the cause has to be sought elsewhere as will be discussed in the next section.

5.14.3.4 Temporal Variations in the Dole Effect

The past history of atmospheric gases can be reconstructed from air bubbles trapped in ice cores, revealing useful information about biogeochemistry and climate. The pioneering ice core study of the isotopes of O_2 by Michael Bender (Bender et al., 1985) showed an enriched value of $\delta^{18}O_{atm}$ in the past glacial period, roughly as expected from the +1‰ higher seawater $\delta^{18}O$ at that time. Past seawater $\delta^{18}O$ is inferred from the $\delta^{18}O$ of benthic foraminifera calcite with appropriate corrections for temperature effects (Waelbroeck et al., 2002), and past values of the DE can be estimated from the difference between the measured ice core $\delta^{18}O_{atm}$ and the reconstructed seawater $\delta^{18}O$.

Subsequently, refinements to the precision of the ice core gas technique and longer ice core records showed that the DE also changes over time (Bender et al., 1994; Malaize et al., 1999). These changes seemed to have a strong precessional (~23 ky) periodicity and were thought to be partly due to low-latitude hydrologic cycle variations, stemming both from the isotopic composition of the rainfall and the relative humidity (which controls the amount of evaporative enrichment of chloroplast water; Farquhar et al., 2007). Heavy convective rains and high humidity both tend to decrease the $\delta^{18}O$ of photosynthetic substrate water. Mélieres et al. (1997) pointed out that a minimum in the DE occurred at 175 ka coincident with a strong North African monsoon and strong precession-driven June insolation. This particular case was instructive because it occurred during a glacial period when boreal and temperate ecosystems were quiescent (Masson et al., 2000).

It now appears likely that the DE is primarily modulated over time by variations in the strength of the low-latitude northern hemisphere monsoon systems (Landais et al., 2010),

Table 6 Calculation of the Dole effect

	$\delta^{18}O$ (vs. VSMOW), $^{18}\varepsilon$ or DE_x (all in ‰)	*Fraction of global O_2 production*	*References*
Marine Dole effect			
$DE_{surface}$	25.2 ± 1.9	0.33	This chapter
DE_{deep}	23.2 ± 0.5	0.04	Luz and Barkan (2011)
DE_{mar}	24.3[a] ± 2.0	0.37	
Terrestrial Dole effect			
$\delta^{18}O$ of photosynthetic O_2	6.5 ± 2.1		West et al. (2008)
Total respiratory fractionation	17.7 ± 1.0		Landais et al. (2007a)
ε_{eq} of O_2 leaf water relative to air	0.75[b] ± 0.05		Benson and Krause (1984)
DE_{terr}	23.5[c] ± 2.3	0.63	
Stratospheric isotopic effect (ε_{strat})	0.3[d] ± 0.1		Luz et al. (1999)
Calculated global Dole effect	23.5[e] ± 2.5		
Measured global Dole effect	23.88 ± 0.02		Barkan and Luz (2005)

[a] 24.3 = (0.33*24.2 + 0.04*23.2)/0.37.
[b] 0.75 is an average for possible temperature-dependent values ranging from 0.7 to 0.8‰.
[c] 23.5 = 6.5 + 17.7 − 0.75.
[d] Calculated from eqn [10] and $^{17}\Delta$ of 0.166‰ (Section 5.14.2) and assuming in the first approximation $\delta^{17}O = \delta^{18}O$, the authors obtain $0.166 = \delta^{18}O - 0.516*\delta^{18}O$, and $\delta^{18}O = \sim 0.3$‰.
[e] 23.5 = 24.3*0.37 + 23.5*0.63 − 0.3.

with strong summer (wet phase) monsoons causing a smaller DE (**Figure 8**). During the Holocene, further support for this monsoon hypothesis is provided by the observed excellent correlation ($R = 0.95$) of the Chinese cave calcite $\delta^{18}O$ with the inferred fractionation that gives rise to the DE (Severinghaus et al., 2009). As the monsoon strength has long been known to be affected by northern hemisphere low-latitude summer insolation (Kutzbach, 1981), it comes as no surprise that the DE has a strong inverse correlation to 30° N summer solstice insolation.

Perhaps more surprising is that the DE also varies with the abrupt millennial-scale oscillations known as Heinrich and Dansgaard–Oeschger events (**Figure 9**; Landais et al., 2007b; Severinghaus et al., 2009), as do the Chinese cave records that are thought to be related to monsoon strength (Cheng et al., 2009; Wang et al., 2001). The abrupt monsoon variations may be related to rapid southward shifts of tropical rainfall belts and the Intertropical Convergence Zone, in response to abrupt increases in northern high-latitude winter sea ice cover (Cheng et al., 2009; Chiang and Bitz, 2005; Wang et al., 2007). However, some caution is required as the exact cause of the Chinese cave isotopic variations is still not understood, and it is possible that they do not solely record summer monsoon rainfall intensity (Clemens et al., 2010).

A third factor that probably contributes to the link between the DE and monsoons, more recently identified (Angert et al., 2003a; **Section 5.14.3.2.1**), is the weak respiratory fractionation characteristic of wet tropical soils. This study also found strong respiratory fractionation in boreal soils, which by itself should cause a positive contribution to the DE. However, boreal precipitation is quite depleted in ^{18}O, causing the opposite effect.

In summary, the low $\delta^{18}O$ of precipitation in heavy summer monsoon rains, the weak evaporative enrichment of leaf water in conditions of high relative humidity, and the weak respiratory fractionation probably all contribute to the observed monsoon–DE linkage, although it is difficult to quantify the relative importance of each factor. The constructive interference of respiratory and hydrologic fractionation at low latitudes, versus their destructive interference at high latitudes, may operate as a sort of 'monsoon rectifier effect' that causes low-latitude hydrology to dominate the variability in the DE (Luz and Barkan, 2011; Severinghaus et al., 2009).

On longer timescales (using the full 800 ky record now available from ice cores; **Figure 8**), there appears to be a broad 100 ky peak in the power spectrum of DE variations, and the DE reaches a maximum every time that a glacial termination occurs (Landais et al., 2010). This likely stems from the fact that the Asian and African monsoons are extremely weak during the times when the northern ice sheets are melting, probably due to winter sea ice cover on the North Atlantic Ocean (Cheng et al., 2009). On even longer timescales, there

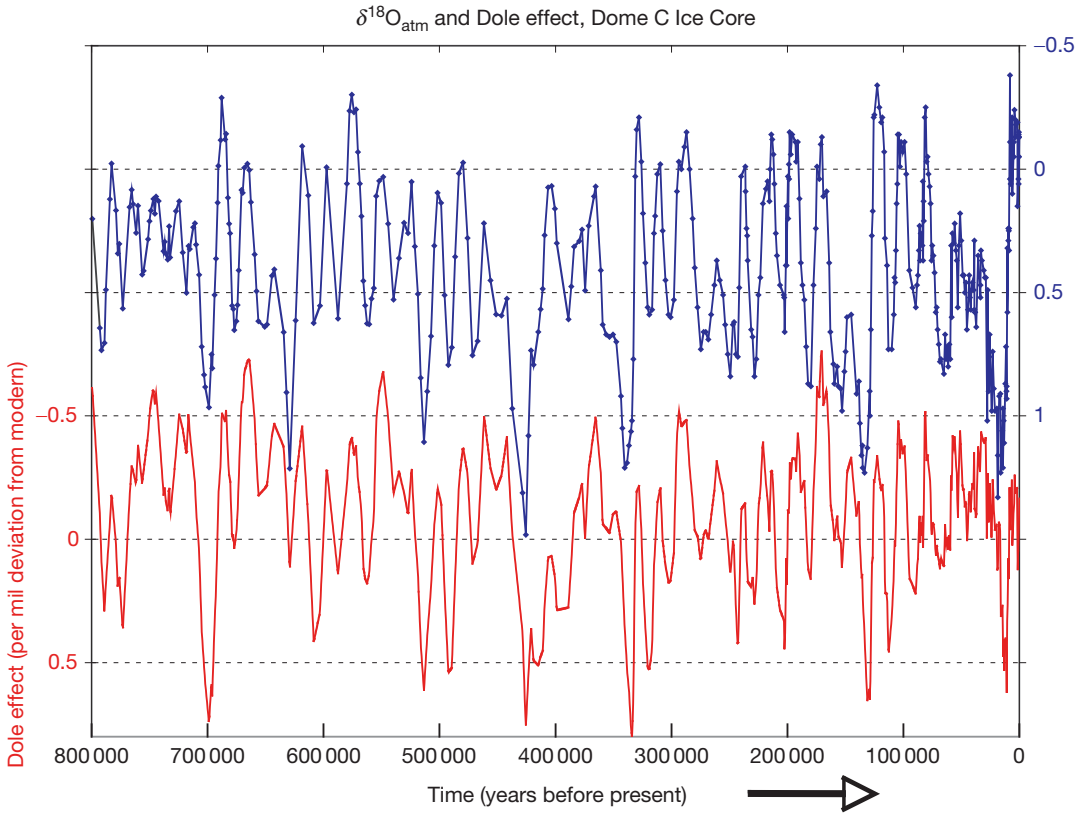

Figure 8 Past variations in the Dole effect (DE) reconstructed from measurements of $\delta^{18}O_{atm}$ in the EPICA Dome C ice core from Antarctica (Landais et al., 2010). Values are plotted using the modern atmosphere as a reference, with inverted axes (following convention) and with time proceeding toward the right. Note the strong precessional (~23 ky) periodicity in the record.

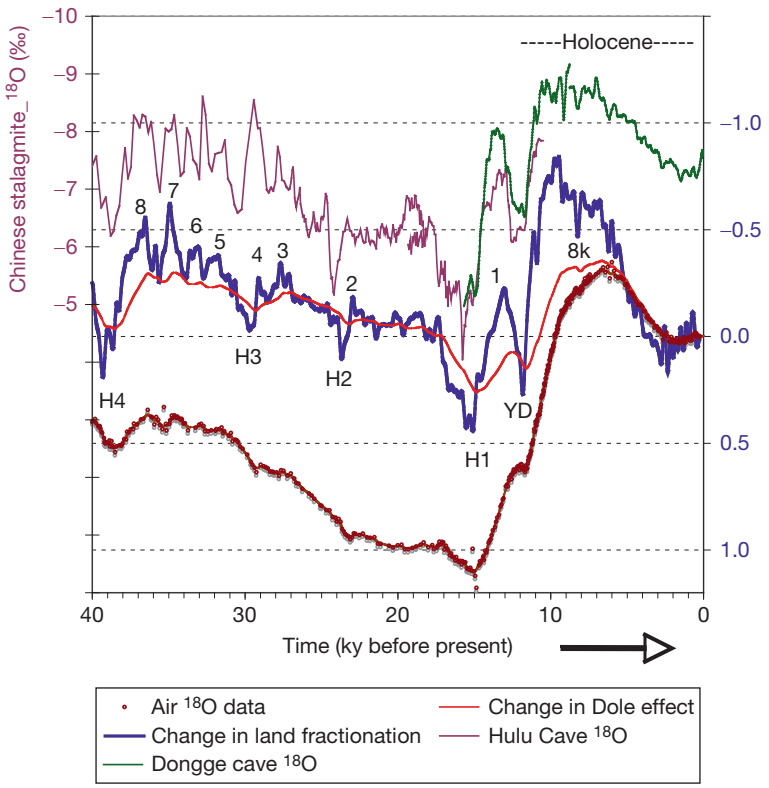

Figure 9 Observed variations in the Dole effect (DE) over the past 40 000 years, from the Siple Dome ice core, Antarctica (Severinghaus et al., 2009). The derivative of the observed DE curve was used to infer the change in land fractionation ($\Delta\varepsilon_{LAND}$), effectively the main driver of changes in the DE (shown in the purple curve). Note the strong similarity with the Chinese cave records, which are thought to reflect monsoon variations (Dykoski et al., 2005; Wang et al., 2001, 2005). Abrupt climate events including Dansgaard–Oeschger events (numbered 1–8), Heinrich events (H1–H4), Younger Dryas (YD), and 8.2 ka event (8k) are shown.

seems to be a tendency for the DE to be larger during times of small eccentricity, such as the interval between 350 and 450 ka (Landais et al., 2010). Interestingly, power spectra show that there is virtually no signal of obliquity in the DE; rather, it is dominated by the precession signal (Landais et al., 2010).

One potential clue about the origin of DE variations comes from direct measurements over the past several decades of the $\delta^{18}O$ of atmospheric CO_2 (Welp et al., 2011). This tracer shares in common with the DE a strong dependence on the $\delta^{18}O$ of chloroplast water because atmospheric CO_2 diffuses rapidly in and out of the stomata of terrestrial plants, rapidly exchanging its isotopes with chloroplast water thanks to the enzyme CA (Farquhar et al., 2007). However, CO_2 has an atmospheric turnover time of the order of 0.5 year in contrast to the ~1000 year turnover time of O_2, making CO_2 a much more sensitive tracer of chloroplast water variations. The CO_2 isotope record shows clearly that during Indonesian drought events, such as accompany El Niño events, chloroplast water becomes isotopically heavy. Thus, the implication is that a weakening of the Indonesian Low, or an increase in the frequency of El Niños, should cause an increase in the DE (Welp et al., 2011). The paucity of El Niños in the early Holocene is consistent with the weak DE during that time. Unfortunately, the CO_2 $\delta^{18}O$ is not well preserved in ice cores due to isotopic exchange with the ice, so it is not possible to reconstruct this tracer back in time.

5.14.4 Oxygen-17 and Oxygen-18 in Atmospheric O_2

5.14.4.1 Mass-Independent Fractionation and Biological Normalization

A new field in stable isotope geochemistry was born when Thiemens and Heidenrich (1983) discovered mass-independent isotopic fractionation in the formation of ozone from O_2 gas by electrical discharge. In their experiment, ozone became equally enriched in both ^{17}O and ^{18}O with respect to the starting O_2, while in the remaining O_2, both isotopes became equally depleted. This experimental result was followed by experiments in which mass-independent fractionation was demonstrated with UV radiation (e.g., Thiemens and Jackson, 1987). In addition, observations on $\delta^{17}O$ and $\delta^{18}O$ of stratospheric ozone and CO_2 showed that both were enriched in ^{17}O and ^{18}O in a mass-independent way (e.g., Boering et al., 2004; Lammerzahl et al., 2002; Mauersberger, 1987). Efforts to explain the chemical origin of mass-independent fractionation started in 1983, but it has taken some two decades before a rigorous theory started to develop (e.g., Hathorn and Marcus, 2001; Marcus, 2004). The theoretical aspects of mass-independent fractionation are beyond the scope of this chapter, and interested readers are referred to a review by Thiemens (2006).

The current understanding of the stratospheric observations is based on the photochemical model of Yung et al. (1991, 1997), where the anomalous ozone enrichment is transferred to CO_2. In this model, ultraviolet photolysis of ozone in the

stratosphere generates an electronically excited oxygen atom ($O(^1D)$), which can undergo isotopic exchange with CO_2 through a transition state (CO_3^*):

$$O_3 + h\nu \rightarrow O(^1D) + O_2$$

$$O(^1D) + CO_2 \rightarrow CO_3^*$$

$$CO_3^* \rightarrow CO_2 + O(^3P)$$

Bender et al. (1994) suggested that because the ultimate source of the oxygen in O_3 and $O(^1D)$ in the stratosphere is the O_2 reservoir, this reservoir must become anomalously depleted as CO_2 becomes anomalously enriched. The stratospheric enrichment in CO_2 is rapidly lost at the Earth's surface by isotope exchange with liquid water in leaves and also in the ocean. In contrast, O_2 does not exchange isotopes with water directly, and the depletion disappears only through the consumption of O_2 by respiration and its replacement by photosynthesis. Yet, the respiratory and photosynthetic fluxes are relatively small in comparison to the stratospheric production, and Bender et al. (1994) suggested that the anomalous depletion should accumulate to a measurable level of about 200 per meg over the 1200 year residence time of atmospheric O_2. Among other factors discussed in the succeeding text, the extent of this anomalous depletion depends on the intensity of UV radiation in the stratosphere, the concentration of atmospheric CO_2, and the rate of global gross O_2 production. Assuming the former factors are known, it should be possible to estimate global gross O_2 production from measurements of the ^{17}O anomaly in air occluded in polar ice cores, which will be discussed in **Section 5.14.4.2**.

Luz et al. (1999) set up an experiment for testing Bender's hypothesis, but before this experiment can be discussed, it is necessary to give some background on definitions of mass-independent anomalies, and for details on triple isotope systematic, the reader is referred to **Section 5.14.2.2** in this chapter. In studies of mass-independent fractionation in ozone and CO_2 in both stratospheric observations and laboratory experiments, the isotopic standards used are VSMOW or CO_2 in equilibrium with VSMOW, and ^{17}O anomalies are calculated, assuming that a $\delta^{17}O/\delta^{18}O$ ratio (or λ; see **Section 5.14.2.2**) of about 0.52 represents normal mass-dependent fractionation. In such studies, the anomaly is calculated as $\Delta^{17}O = \delta^{17}O - \lambda^*\delta^{18}O$ ($\lambda = \sim 0.52$) and its magnitude varies over ranges of several per mil or more. For such large variations, most Earth materials, excluding certain stratospheric gases, can be considered as being affected by mass-dependent fractionations and are thus defined 'normal.' However, the magnitude of the negative mass-independent fractionation in atmospheric O_2 or of oceanic dissolved O_2 is very small and must be treated more rigorously, and both standards and values of λ should be chosen such that they optimally fit the case being studied.

The standard of choice for studies of O_2 gas is present atmospheric O_2 (Luz and Barkan, 2005). Yet, as discussed earlier, this standard is not 'normal' in that it is deficient in ^{17}O. So $^{17}\Delta$ as defined in eqn [10] (**Section 5.14.2**) is zero for atmospheric O_2 and has a positive value for O_2 produced by photosynthesis from natural water. As for values of λ, the best choice is for those of dark respiration which is the most ubiquitous O_2 uptake mechanism on Earth. Depending on whether the application is for estimation of marine gross O_2 production (see succeeding text) or global gross O_2 production, the optimal values of λ are 0.518 and 0.516, respectively (Luz and Barkan, 2005).

The experiment of Luz et al. (1999) was run in an airtight terrarium that contained *Philodendron* plant, soil, and natural meteoric water. The terrarium was illuminated by artificial light with no UV radiation. Inside the terrarium, O_2 production and consumption occurred by the plant and by soil microorganisms. The experiment started with atmospheric air in the terrarium. As the experiment progressed, the initial atmospheric O_2 was partially consumed by respiration and gradually replaced by newly produced photosynthetic O_2. The isotopic composition of O_2 in the terrarium was monitored and $^{17}\Delta$ was calculated from $\delta^{17}O$ and $\delta^{18}O$ measurements. The results from one of the experiments are shown in **Figure 10** and show an initial gradual increase in $^{17}\Delta$, and then the values level off indicating that O_2 in the terrarium was completely replaced with new oxygen of biological origin alone with no effects of UV radiation. As can be seen, the $^{17}\Delta$ of this bio-O_2 has reached a maximum value designated $^{17}\Delta_{bio}$ ($^{17}\Delta_{max}$ in various previous publications). In the experiment shown in **Figure 10**, $^{17}\Delta_{bio}$ is about 150 per meg. Bio-O_2 is considered 'normal' because it has lost the anomalous photochemical signature that atmospheric O_2 contains.

Depending on the experimental conditions and the water substrate from which photosynthesis makes O_2, there is a range of various 'normal' bio-O_2s. For example, experiments similar to that described earlier have been carried out with marine organisms in aquaria and the average value of $^{17}\Delta_{bio}$ in these latter experiments was 249 per meg (Barkan and Luz, 2011; Luz and Barkan, 2000). In **Figure 11**, it is shown schematically how $^{17}\Delta_{bio}$ is attained in such experiments.

In the open ocean, a simple steady-state situation where respiration and photosynthesis produce bio-O_2 and gas exchange tends to bring $^{17}\Delta$ of dissolved O_2 ($^{17}\Delta_{dis}$) to equilibrium with the atmosphere ($^{17}\Delta_{eq}$) may be considered. In this case, measurements of $^{17}\Delta_{dis}$ indicate the ratio of gross O_2 production with isotopic composition of $^{17}\Delta_{bio}$ to air–sea gas exchange introducing dissolved O_2 with isotopic composition of $^{17}\Delta_{eq}$. Luz and Barkan (2000) introduced a method in which gross O_2 production could be estimated from measurements of $^{17}\Delta_{dis}$ and the rate of air–gas exchange. This method has been applied all over the ocean (e.g., Hendricks et al., 2004; Quay et al., 2010; Reuer et al., 2007; Sarma et al., 2008). Recently, Prokopenko et al. (2011) improved the method by obtaining a

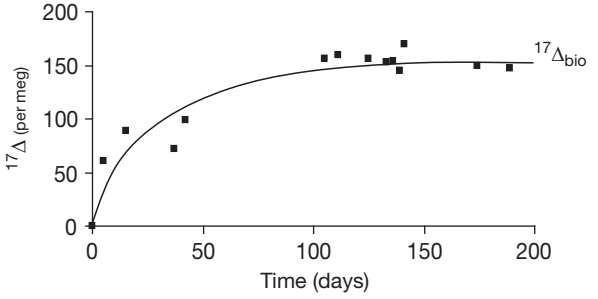

Figure 10 Removal of the mass-independent signature from atmospheric O_2 in a terrarium experiment.

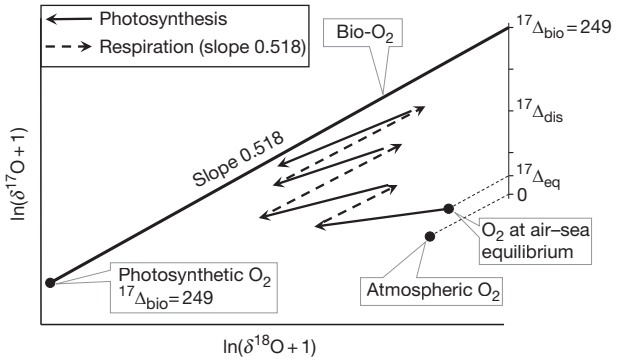

Figure 11 Schematic illustration (not to scale) showing how photosynthesis and respiration affect $\delta^{18}O$, $\delta^{17}O$, and $^{17}\Delta$ of dissolved O_2 ($^{17}\Delta_{dis}$). Newly produced photosynthetic O_2 mixes with the existing O_2, and depending on the extent of photosynthesis, the mixture isotopic composition will move toward that of seawater (solid arrows, which are slightly curved as in **Figure 3**) and $^{17}\Delta_{dis}$ increases. Respiration (dashed arrows) increases both $\delta^{18}O$ and $\delta^{17}O$ but does not change $^{17}\Delta_{dis}$ because $\ln(\delta^{17}O+1)/\ln(\delta^{18}O+1)=0.518$. With sufficient photosynthesis and respiration cycles, $^{17}\Delta_{dis}$ will approach $^{17}\Delta_{bio}$. From this point on, photosynthesis will decrease both $\delta^{18}O$ and $\delta^{17}O$ and respiration will increase them but $^{17}\Delta_{dis}$ will not change and its value will remain equal to $^{17}\Delta_{bio}$.

rigorous equation for the steady-state case. This equation has been applied by Luz and Barkan (2011b) for the calculation of $^{18}\varepsilon_{up}$ as described in **Section 5.14.3.2.2**.

Returning to measurements of $^{17}\Delta_{bio}$, the different values in aquarium experiments with seawater and terrarium experiments with freshwater cannot be explained from interplay between mass-independent fractionation and mass-dependent effects because in both types of experiments there was no UV radiation. Instead, the cause of the difference in the values of $^{17}\Delta_{bio}$ is that several mass-dependent processes having somewhat different $^{17}\varepsilon/^{18}\varepsilon$ ratios come into play. The main controlling factors in aquarium experiments with seawater are the isotopic composition of the water and ordinary respiration with only a small effect of fractionation in photosynthesis (Barkan and Luz, 2011). On the other hand, in the terrarium experiments, the substrate water came from natural meteoric water that was affected by hydrologic processes of evaporation and precipitation. An extensive survey and discussion of these processes is found in Luz and Barkan (2010). Briefly, the hydrologic cycle starts from oceanic evaporation with an excess of ^{17}O ($^{17}O_{excess}$) of about 33 per meg with respect to seawater, but the $^{17}\varepsilon/^{18}\varepsilon$ ratio in vapor liquid equilibrium, which governs precipitation, is larger than in respiration. Consequently, $^{17}\Delta_{bio}$ in the terrarium experiment of Luz and Barkan (2005) was smaller (194 per meg) than in seawater (249 per meg). It is noted that there is no one universal value for all meteoric waters, and in general, if terrarium experiments were run with water having lower $\delta^{18}O$ than in the experiment of Luz and Barkan (2005), the resulting $^{17}\Delta_{bio}$ would have been smaller than 194 per meg.

In the natural terrestrial biosphere, the situation is more complex because in contrast to the terrarium, air relative humidity is less than 100% and due to transpiration into low humidity air, leaf water becomes enriched in both ^{17}O and ^{18}O in comparison to meteoric water. Landais et al. (2006) studied the isotopic effects of transpiration and their impact on $\delta^{17}O$ and $\delta^{18}O$ of atmospheric O_2. These studies showed that the $\ln(^{17}\alpha)/\ln(^{18}\alpha)$ ratio in transpiration is considerably smaller than in global meteoric waters and despite the enrichment in ^{18}O in this process that significantly increases $\delta^{18}O$ of global leaf water (see **Section 5.14.3.2.3**), its $^{17}O_{excess}$ goes down with respect to seawater. But it is noted that in calculations of $^{17}O_{excess}$ in hydrology, λ is 0.528, while in global calculations of $^{17}\Delta$, it is 0.516, which is quite similar to λ in global transpiration (0.517, Landais et al., 2007a). Therefore, in O_2 emission from the terrestrial biosphere, $^{17}\Delta_{bio}$ becomes smaller and smaller as $\delta^{18}O$ of meteoric water goes low, while transpiration only slightly increases its value. The effects of the hydrologic cycle and leaf transpiration are shown schematically in **Figure 12**.

A further complication in terrestrial systems arises from CO_2 limitation and the resulting consumption of O_2 by photorespiration. This was demonstrated by Angert et al. (2003b) who showed that $^{17}\Delta_{bio}$ in a terrarium experiment became about 100 per meg when experiments were carried out at continuous illumination that caused CO_2 concentration to go below 500 ppmv. In contrast, experiments with the same terrarium, plant, soil, and water, but with changing light–dark cycles and CO_2 remaining always above 2000 ppmv, yielded $^{17}\Delta_{bio}$ of 194 per meg (Luz and Barkan, 2005). Indeed, direct measurements by *in vitro* experiments of Helman et al. (2005; summarized in **Table 1**) demonstrated that $^{17}\varepsilon/^{18}\varepsilon$ ratio of O_2 uptake by glycolate oxidase, an important reaction in photorespiration, was 0.501 and significantly smaller than in dark respiration (0.518).

Landais et al. (2007a) used the information on photorespiration and fractionation in the hydrologic cycle and in transpiration and calculated $^{17}\Delta_{bio}$ of the terrestrial biosphere as 110 ± 35 per meg with respect to atmospheric O_2. At the time of their publication, information on $^{17}O_{excess}$ of meteoric water was not available. It is now known that meteoric waters have $^{17}O_{excess}$ of 33 per meg (Luz and Barkan, 2010). On the other hand, $^{17}\Delta$ of seawater with respect to atmospheric O_2 is 223 and not 249 per meg, which is the value of $^{17}\Delta$ produced by photosynthesis from seawater (Barkan and Luz, 2011). These effects are included in **Figure 12**, but an important point is that the $^{17}O_{excess}$ of meteoric water is almost entirely compensated by the lower $^{17}\Delta$ of seawater (223 per meg) than that of photosynthetic O_2 (249 per meg).

In **Figure 12**, it is shown graphically how the various isotopic effects of hydrology and biology are used for deriving the terrestrial and global $^{17}\Delta_{bio}$ as 117 ± 35 and 166 ± 51 per meg, respectively. Evidently, there is considerable uncertainty in these calculated values, but despite that, they are useful for gaining insight on the increase of global gross O_2 production since the Last Glacial Maximum (LGM).

5.14.4.2 Temporal Variations in $^{17}O/^{16}O$ and $^{18}O/^{16}O$

The number of studies on past variations of $^{17}\Delta$ in atmospheric O_2 is small. The first measurements were done by Luz et al. (1999) on samples of air extracted from the GISP-2 ice core that had been drilled in Summit, Greenland. This record spans the last 82 000 years. A more detailed study on the same core was

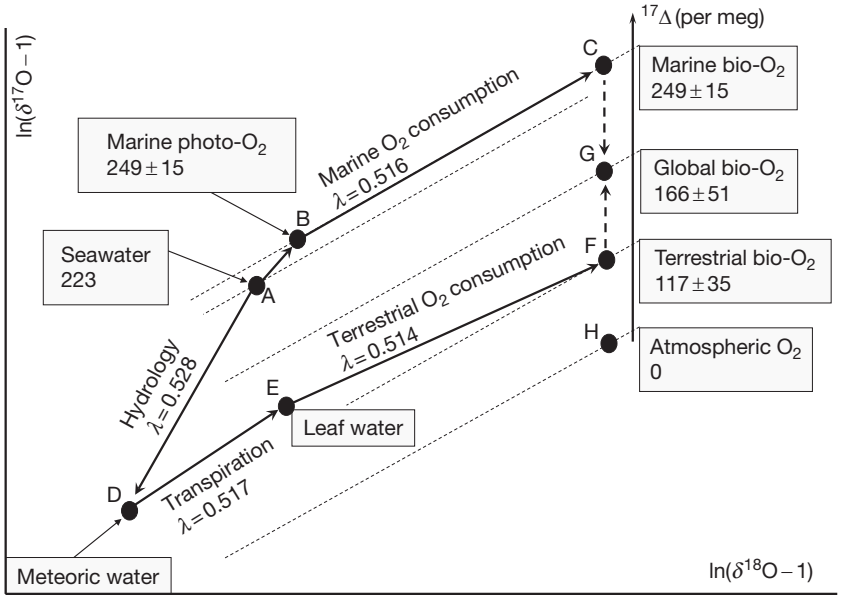

Figure 12 Schematic illustration of processes affecting the $^{17}\Delta$ of atmospheric O_2. In order to show the variations in line slopes and $^{17}\Delta$ values, the $\ln(\delta^{17}O+1)$ scale is highly exaggerated and is not uniform. Both axes are not drawn to scale. $^{17}\Delta$ values are constant along the dashed lines with slope of 0.516. The slope of arrow AB is 0.521.

published by Blunier et al. (2002) and showed the same trends in $^{17}\Delta$. In general, during the LGM, atmospheric O_2 was about 40 per meg higher in $^{17}\Delta$ than the present atmosphere. During the rest of the last glacial, $^{17}\Delta$ varied around an average value of about 30 per meg. In a much more indirect way, Bao et al. (2008) suggested that $\delta^{17}O$ and $\delta^{18}O$ of sulfate in barites and evaporites from the early Cambrian reflect, in part, the isotopic composition of the atmosphere of that time. Cast in terms of $^{17}\Delta$ as defined in this chapter, the maximum deviations they reported were about −700 per meg with respect to the present atmosphere. Because, as they proposed, only 5–20% of the sulfate oxygen was of atmospheric origin, it is calculated that $^{17}\Delta$ of the early Cambrian air reached an extremely low level of −14 000 per meg or −14‰ with respect to today's air.

Before explaining the origin of these past variations in $^{17}\Delta$, it should be recognized that in addition to biological and photochemical controls, abundances of isotopes and elements of air occluded in ice cores are affected by gravitational and thermal diffusion fractionations (e.g., Severinghaus et al., 1998). The records presented by Luz et al. (1999) and Blunier et al. (2002) were corrected for gravitational fractionations by subtraction of measured $\delta^{15}N$ of N_2 in the same samples from the measured $\delta^{17}O$ and by subtraction of $2(\delta^{15}N)$ from the measured $\delta^{18}O$. The size of the correction is on the order of 10–15 per meg in $^{17}\Delta$.

Following Luz et al. (1999), $^{17}\Delta$ of oxygen in the atmosphere, $^{17}\Delta_{atm}$, can be expressed as

$$F_{bio} \times (^{17}\Delta_{bio} - {}^{17}\Delta_{atm}) = F_{strat} \times (^{17}\Delta_{strat} - {}^{17}\Delta_{atm}) \quad [17]$$

where $^{17}\Delta_{strat}$ and $^{17}\Delta_{bio}$ are the $^{17}\Delta$ of stratospheric O_2 flux (F_{strat}) and the biological O_2 flux (F_{bio}), respectively. The ratio of the global gross O_2 production between the LGM and the present is calculated from eqn [18] as (Landrais et al., 2007a)

$$\frac{F_{bio,LGM}}{F_{bio,PST}} = \frac{F_{strat,LGM} \times (^{17}\Delta_{strat,LGM} - {}^{17}\Delta_{atm,LGM})}{F_{strat,\ PST} \times (^{17}\Delta_{strat,PST} - {}^{17}\Delta_{atm,PST})} \times \frac{(^{17}\Delta_{bio,PST} - {}^{17}\Delta_{atm,PST})}{(^{17}\Delta_{bio,LGM} - {}^{17}\Delta_{atm,LGM})} \quad [18]$$

By definition, $^{17}\Delta_{atm,PST} = 0$, and $^{17}\Delta_{atm,LGM}$ was determined by Blunier et al. (2002) as +43 per meg (note that the original value of Blunier et al. (2002) is +38 per meg since it was calculated with λ of 0.521 instead of 0.516, which is the optimal value for global calculations).

Luz et al. (1999) and Blunier et al. (2002) assumed that the ratio of the production rates of anomalously depleted O_2 in the stratosphere, $F_{strat} \times (^{17}\Delta_{strat} - {}^{17}\Delta_{atm})$, between the LGM and the present is proportional to the ratio of atmospheric CO_2 concentrations between the LGM and the preindustrial Holocene. This assumption implies that the photochemical reactions involved in the production of CO_2 high in $^{17}\Delta$ and O_2 low in $^{17}\Delta$ are first order with respect to CO_2 concentration. Bao et al. (2008) dealt with this assumption and showed that it is reasonable at least for CO_2 concentration up to about 2000 ppm. With this assumption and using CO_2 concentrations of 280 ppmv for the preindustrial Holocene and 190 ppmv for the LGM (Barnola et al., 1987), eqn [18] becomes

$$\frac{F_{bio,LGM}}{F_{bio,PST}} = \frac{190}{280} \times \frac{^{17}\Delta_{bio,PST}}{(^{17}\Delta_{bio,LGM} - 43)} \quad [19]$$

Clearly, the correction for the different CO_2 concentration between the two periods is large, and indeed, the main driving force for the glacial to postglacial change in $^{17}\Delta$ was the rise in concentration of atmospheric CO_2. **Figure 13** shows the $^{17}\Delta$ of atmospheric O_2 versus CO_2 from the data of Luz et al.

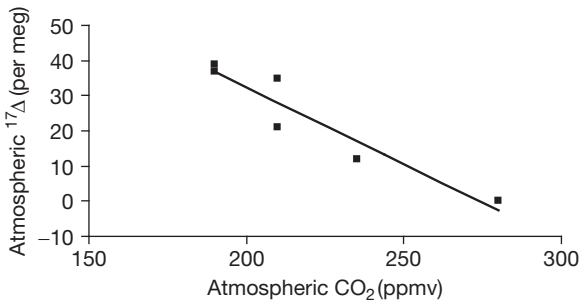

Figure 13 $^{17}\Delta$ versus CO_2 concentration in air extracted from GISP-2 ice core.

(1999) and a similar relation can be shown for Blunier et al. (2002) results.

Before continuing with the ice core record, it is noted that Bao et al. (2008) suggested that extremely high CO_2 concentration (up to 25 000 ppmv) can explain the huge negative $^{17}\Delta$ they measured in early Cambrian sulfates. The same logic was followed by Gehler and Pack (2010) who proposed high atmospheric CO_2, although far less dramatic, in the middle Eocene.

Application of eqn [19] requires that $^{17}\Delta_{bio}$ be known for both the PST and the LGM. Applying, as did Luz et al. (1999), 155 per meg for both, $F_{bio,LGM}/F_{bio,PST}$ is calculated as 0.94. If 249 per meg is applied instead, $F_{bio,LGM}/F_{bio,PST}$ becomes 0.82, and if this ratio is calculated with $^{17}\Delta_{bio,LGM}$ value equal to 214 and the PST value equal to 166 per meg, a ratio of 0.66 is obtained. These simple calculations demonstrate the sensitivity of $F_{bio,LGM}/F_{bio,PST}$ to uncertainty in the value of $^{17}\Delta_{bio}$.

Understanding the importance of reliable $^{17}\Delta_{bio}$ values for estimates of global O_2 production motivated Landais et al. (2006, 2007a) to study the factors controlling them at present and in the last glacial. Their main results on the present $^{17}\Delta_{bio}$ and the differences between land and sea have been reviewed in the previous section, and a global $^{17}\Delta_{bio}$ value of 166 per meg has been derived. However, this value cannot be used for the LGM in which $^{17}\Delta_{bio}$ must have been larger for three main reasons: (1) in the LGM, $^{17}\Delta$ of seawater was larger, (2) $^{17}\Delta$ of meteoric water used by plants at that time was also higher, and (3) smaller contribution of photorespiration led to the emission of O_2 with larger $^{17}\Delta$ by the glacial terrestrial biosphere.

At the LGM, $\delta^{18}O$ of seawater was about 1‰ larger than today (Waelbroeck et al., 2002), and from the understanding of isotope hydrology, there must have been parallel change in $\ln(\delta^{17}O+1)$ and it can be calculated as $0.528*\ln(\delta^{18}O+1)$. Because for global considerations $^{17}\Delta$ is calculated with λ equal 0.516 (see lines of constant $^{17}\Delta$ in **Figure 13**), it can be calculated that this isotopic change in seawater involved a 12 $(=[(0.528-0.516)*\ln(1.0/1000+1)]*10^6)$ per meg increase in $^{17}\Delta_{bio}$ of the glacial ocean.

In a similar way, due to the widespread glaciers, vegetation in the high latitudes of the northern hemisphere was greatly reduced. Landais et al. (2007a) estimated that, on average, $\delta^{18}O$ of meteoric water used by the LGM vegetation was about 1.2‰ higher than at present. Calculating in the same way as earlier, such a shift in $\delta^{18}O$ should have been associated with a 15 per meg increase in LGM leaf water.

Finally, global O_2 uptake via photorespiration was reduced due to a large reduction in the abundance of C_3 vegetation and the increase of the relative abundance of C_4 plants (it is known that C_4 vegetation concentrates CO_2 and therefore suppresses photorespiration). At present, the $\ln(\delta^{17}O+1)/\ln(\delta^{18}O+1)$ in terrestrial O_2 uptake is reduced from 0.516 to 0.514 due to photorespiration. Landais et al. (2007a) calculated that this ratio at the LGM was larger and consequently $^{17}\Delta_{bio}$ was further increased by 15 per meg.

Considering the above, Landais et al. (2007a) estimated that in the LGM the terrestrial $^{17}\Delta_{bio}$ was 30 per meg larger than today and then calculated $^{17}\Delta_{bio}$ estimates for the present as 124–189 per meg and 156–234 per meg for the LGM. Finally, they concluded that $F_{bio,LGM}$ was only 60–75% of $F_{bio,PST}$. Despite the uncertainty, this calculation shows that global gross production at the LGM was substantially smaller than in previous estimates.

The above analysis shows that $^{17}\Delta$ of air from ice cores is useful for estimating past changes in global photosynthetic rates. However, derivation of meaningful conclusions requires careful consideration of hydrology and changes in terrestrial vegetation and their effects on $^{17}\Delta_{bio}$.

References

Aggarwal PK, Dillon MA, and Tanweer A (2004) Isotope fractionation at the soil–atmosphere interface and the ^{18}O budget of atmospheric oxygen. *Geophysical Research Letters* 31: L14202.

Angert A, Barkan E, Barnett B, et al. (2003a) Contribution of soil respiration in tropical, temperate, and boreal forests to the ^{18}O enrichment of atmospheric O_2. *Global Biogeochemical Cycles* 17(3): 1089.

Angert A and Luz B (2001) Fractionation of oxygen isotopes by root respiration: Implications for the isotopic composition of atmospheric O_2. *Geochimica et Cosmochimica Acta* 65: 1679–1703.

Angert A, Luz B, and Yakir D (2001) Fractionation of oxygen isotopes by respiration and diffusion in soils: Implications for the isotopic composition of atmospheric O_2. *Global Biogeochemical Cycles* 14: 871–881.

Angert A, Rachmilevitch S, Barkan E, and Luz B (2003b) Effects of photorespiration, the cytochrome pathway, and the alternative pathway on the triple isotopic composition of atmospheric O_2. *Global Biogeochemical Cycles* 17(1): 1030.

Appenzeller C, Holton JR, and Rosenlof KH (1996) Seasonal variation of mass transport across the tropopause. *Journal of Geophysical Research* 101(D10): 15071–15078.

Assonov SS and Brenninkmeijer CAM (2001) A new method to determine the ^{17}O isotopic abundance in CO_2 using oxygen isotope exchange with a solid oxide. *Rapid Communications in Mass Spectrometry* 15: 2426–2437.

Bader MR, von Caemmerer S, Ruuska S, and Nakano H (2000) Electron flow to oxygen in higher plants and algae: Rates and control of direct photoreduction (Mehler reaction) and rubisco oxygenase. *Philosophical Transactions of the Royal Society, Series B* 355: 1433–1445.

Bailey S, Melis A, Mackey KRM, et al. (2008) Alternative photosynthetic electron flow to oxygen in marine *Synechococcus*. *Biochimica et Biophysica Acta – Bioenergetics* 1777: 269–276.

Bao H, Lyons J, and Zhou C (2008) Triple oxygen isotope evidence for elevated CO_2 levels after a Neoproterozoic glaciation. *Nature* 453: 504–506.

Barkan E and Luz B (2003) High-precision measurements of $^{17}O/^{16}O$ and $^{18}O/^{16}O$ of O_2 and O_2/Ar ratio in air. *Rapid Communications in Mass Spectrometry* 17: 2809–2814.

Barkan E and Luz B (2005) High precision measurements of $^{17}O/^{16}O$ and $^{18}O/^{16}O$ of O_2 in H_2O. *Rapid Communications in Mass Spectrometry* 19: 3737–3742.

Barkan E and Luz B (2007) Diffusivity fractionations of $H_2{}^{16}O/H_2{}^{17}O$ and $H_2{}^{16}O/H_2{}^{18}O$ in air and their implications for isotope hydrology. *Rapid Communications in Mass Spectrometry* 21: 2999–3005.

Barkan E and Luz B (2011) The relationships among the three stable isotopes of oxygen in air, seawater and marine photosynthesis. *Rapid Communications in Mass Spectrometry* 25: 2367–2369.

Barnola JM, Raynaud D, Korotkevich YS, and Lorius C (1987) Vostok ice core provides 160,000-year record of atmospheric CO_2. *Nature* 329: 408–414.

Bender ML (1990) The $\delta^{18}O$ of dissolved O_2 in seawater: A unique tracer of circulation and respiration in the deep sea. *Journal of Geophysical Research* 95(C12): 22243–22252.

Bender M, Labeyrie L, Raynaud D, and Lorius C (1985) Isotopic composition of atmospheric O_2 in ice linked with deglaciation and global primary productivity. *Nature* 318: 349–352.

Bender M, Sowers T, and Labeyrie L (1994) The Dole effect and its variations during the last 130,000 years as measured in the Vostok ice core. *Global Biogeochemical Cycles* 8: 363–376.

Bennoun P (1994) Chlororespiration revisited: Mitochondrial–plastid interactions in *Chlamydomonas*. *Biochimica et Biophysica Acta – Bioenergetics* 1186: 59–66.

Benson BB and Krause DK Jr. (1984) The concentration and isotopic fractionation of oxygen dissolved in freshwater and seawater in equilibrium with atmosphere. *Limnology and Oceanography* 29: 620–632.

Bigeleisen L (1952) The effects of isotopic substitutions on the rates of chemical reactions. *Journal of Physical Chemistry* 56: 823–828.

Bigeleisen L and Wolfsberg M (1958) Theoretical and experimental aspects of isotope effects in chemical kinetics. *Advances in Chemical Physics* 1: 15–76.

Blunier T, Barnett B, Bender ML, and Hendricks MB (2002) Biological oxygen productivity during the last 60,000 years from triple oxygen isotope measurements. *Global Biogeochemical Cycles* 16(3): 1029.

Boering KA, Jackson T, Hoag KJ, et al. (2004) Observations of the anomalous oxygen isotopic composition of carbon dioxide in the lower stratosphere and the flux of the anomaly to the troposphere. *Geophysical Research Letters* 31: L03109.

Bottinga Y and Craig H (1969) Oxygen isotope fractionation between COP and water and the isotopic composition of marine atmosphere. *Earth and Planetary Science Letters* 5: 285–295.

Bowen GJ and Revenaugh J (2003) Interpolating the isotopic composition of modern meteoric precipitation. *Water Resources Research* 39(10): 1299.

Brenninkmeijer CAM, Kraft P, and Mook WG (1983) Oxygen isotope fractionation between CO_2 and H_2O. *Isotope Geoscience* 1: 181–190.

Broecker WS (1970) Man's oxygen reserves. *Science* 168: 1537–1538.

Cheng H, Edwards RL, Broecker WS, et al. (2009) Ice age terminations. *Science* 326: 248–252.

Chiang JCH and Bitz CM (2005) Influence of high latitude ice cover on the marine intertropical convergence zone. *Climate Dynamics* 25(5): 477–496.

Clayton RN, Grossman L, and Mayeda TK (1973) A component of primitive nuclear composition in carbonaceous meteorites. *Science* 182: 485–498.

Clemens SC, Prell WL, and Sun Y (2010) Orbital-scale timing and mechanisms driving Late Pleistocene Indo-Asian summer monsoons: Reinterpreting cave speleothem $d^{18}O$. *Paleoceanography* 25: PA4207.

Coplen TB (1994) Reporting of stable hydrogen, carbon and oxygen isotope abundances. *Pure and Applied Chemistry* 66: 273–276.

Coplen TB, Kendall C, and Hopple J (1983) Comparison of stable isotope references samples. *Nature* 302: 236–238.

Dansgaard W (1964) Stable isotopes in precipitation. *Tellus* 16: 436–468.

Dole M (1935) The relative atomic weight of oxygen in water and in air. *Journal of the American Chemical Society* 57: 2731.

Dole M (1965) The natural history of oxygen. *Journal of General Physiology* 49: 5–27.

Dole M and Jenks G (1944) Isotopic composition of photosynthetic oxygen. *Science* 100: 409.

Dongmann G (1974) The contribution of land photosynthesis to the stationary enrichment of ^{18}O in the atmosphere. *Radiation and Environmental Biophysics* 11: 219–225.

Dongmann G, Forstel H, and Wagener K (1972) ^{18}O-rich oxygen from land photosynthesis. *Nature New Biology* 240: 127–128.

Dykoski CA, Edwards RL, Cheng H, et al. (2005) A high-resolution, absolute-dated Holocene and deglacial Asian monsoon record from Dongge Cave, China. *Earth and Planetary Science Letters* 233: 71–86.

Eisenstadt D, Barkan E, Luz B, and Kaplan A (2010) Enrichment of oxygen heavy isotopes during photosynthesis in phytoplankton. *Photosynthesis Research* 103: 97–103.

Farquhar GD, Cernusak LA, and Barnes B (2007) Heavy water fractionation during transpiration. *Plant Physiology* 143: 11–18.

Farquhar GD and Lloyd J (1993) Carbon and oxygen isotope effect in the exchange of carbon dioxide between terrestrial plants and the atmosphere. In: Ehleringer JR (ed.) *Stable Isotopes and Plant Carbon–Water Relations*, pp. 47–70. San Diego, CA: Academic Press.

Farquhar GD, Lloyd J, Taylor JA, et al. (1993) Vegetation effects on the isotope composition of oxygen in atmospheric CO_2. *Nature* 363: 439–443.

Farquhar GD, O'Leary MH, and Berry JA (1982) On the relationship between carbon isotope discrimination and the intercellular carbon dioxide concentration in Leaves. *Australian Journal of Plant Physiology* 9: 121–137.

Francey R and Tans P (1987) Latitudinal variation in ^{18}O of atmospheric CO_2. *Nature* 327: 495–497.

Gamo T, Tsutsumi M, Sakai H, et al. (1989) Carbon and oxygen isotopic ratios of carbon dioxide of a stratospheric profile over Japan. *Tellus B* 41: 127–133.

Gat JR (1996) Oxygen and hydrogen isotopes in the hydrologic cycle. *Annual Review of Earth and Planetary Sciences* 24: 225–262.

Gehler A and Pack A (2010) Cenozoic and Mesozoic atmospheric carbon dioxide concentrations from triple oxygen isotope analyses of mammalian bioapatite. *Geophysical Research Abstracts* 12: EGU2010-14059.

Gillon J and Yakir D (2001) Influence of carbonic anhydrase activity in terrestrial vegetation on the ^{18}O content of atmospheric CO_2. *Science* 291: 2584–2587.

Gonfiantini R (1978) Standards for stable isotope measurements in natural compounds. *Nature* 271: 534–536.

Gonfiantini R, Gratzui S, and Tongiorgi E (1965) Oxygen isotopic composition of water in leaves. *Isotopes and Radiation in Soil–Plant Nutrition Studies*, pp. 405–410. Vienna: IAEA.

Guy RD, Berry JA, Fogel ML, and Hoering TC (1989) Differential fractionation of oxygen isotopes by cyanide-resistant and cyanide-sensitive respiration in plants. *Planta* 177: 483–491.

Guy RD, Berry JA, Fogel ML, Turpin DH, and Weger HG (1992) Fractionation of the stable isotopes of oxygen during respiration by plants – The basis of a new technique to estimate partitioning to the alternative path. In: Lambers H and Van der Plas LHW (eds.) *Biochemical and Physiological Aspects of Plant Respiration*, pp. 443–453. The Hague: SPB Academic Publishing.

Guy RD, Fogel ML, and Berry JA (1993) Photosynthetic fractionation of the stable isotopes of oxygen and carbon. *Plant Physiology* 101: 37–47.

Hathorn BC and Marcus RA (2001) Estimation of vibrational frequencies and vibrational densities of states in isotopically substituted nonlinear triatomic molecules. *Journal of Physical Chemistry* 105: 5586–5589.

Helman Y, Barkan E, Eisenstadt D, Luz B, and Kaplan A (2005) Fractionation of the three stable oxygen isotopes by oxygen-producing and oxygen-consuming reactions in photosynthetic organisms. *Plant Physiology* 138: 2292–2298.

Hendricks MB, Bender ML, and Barnett BA (2004) Net and gross O_2 production in the Southern Ocean from measurements of biological O_2 supersaturation and its triple isotope composition. *Deep Sea Research Part I: Oceanographic Research Papers* 51(11): 1541–1561.

Hendricks MB, Bender ML, Barnett BA, Strutton P, and Chavez FP (2005) Triple oxygen isotope composition of dissolved O_2 in the equatorial Pacific: A tracer of mixing, production, and respiration. *Journal of Geophysical Research* 110: C12021.

Hoffmann G, et al. (2004) A model of the Earth's Dole effect. *Global Biogeochemical Cycles* 18: GB1008.

Holton J (1990) On the global exchange of mass between the stratosphere and troposphere. *Journal of the Atmospheric Sciences* 47: 392–395.

Horibe Y, Shigehara K, and Takakuwa Y (1973) Isotope separation factor of carbon dioxide-water system and isotopic composition of atmospheric oxygen. *Journal of Geophysical Research* 78: 2625–2629.

Jenkins WJ and Goldman JC (1985) Seasonal oxygen cycling and primary production in the Sargasso Sea. *Journal of Marine Research* 43: 465–491.

Juranek LW and Quay PD (2005) In vitro and in situ gross primary and net community production in the North Pacific Subtropical Gyre using labeled and natural abundance isotopes of dissolved O_2. *Global Biogeochemical Cycles* 19: GB3009.

Keeling CD (1961) The concentration and isotopic abundance of carbon dioxide in rural and marine air. *Geochimica et Cosmochimica Acta* 24: 277–298.

Kiddon J, Bender ML, Orchardo J, Caron DA, Goldman JC, and Dennett M (1993) Isotopic respiration of oxygen by respirating marine organisms. *Global Biogeochemical Cycles* 7: 679–694.

Kroopnick PM (1975) Photosynthesis, and oxygen isotope fractionation in oceanic surface water. *Limnology and Oceanography* 20: 988–992.

Kroopnick P and Craig H (1972) Atmospheric oxygen: Isotopic composition and solubility fractionation. *Science* 175: 54–55.

Kroopnick P and Craig H (1976) Oxygen isotope fractionation in dissolved oxygen in the deep sea. *Earth and Planetary Science Letters* 32: 375–388.

Kutzbach J (1981) Monsoon climate of the early Holocene: Climate experiment with Earth's orbital parameters for 9000 years ago. *Science* 214: 59–61.

Lammerzahl P, Rockmann T, and Brenninkmeijer CAM (2002) Oxygen isotope composition of stratospheric carbon dioxide. *Geophysical Research Letters* 29: 23–24.

Landais A, Barkan E, Yakir D, and Luz B (2006) The triple isotopic composition of oxygen in leaf water. *Geochimica et Cosmochimica Acta* 70: 4105–4115.

Landais A, Dreyfus G, Capron E, et al. (2010) What drives the millennial and orbital variations of $\delta^{18}O_{atm}$? *Quaternary Science Reviews* 29: 235–246.

Landais A, Lathiere J, Barkan E, and Luz B (2007a) Reconsidering the change in global biosphere productivity between the Last Glacial Maximum and present day from the triple oxygen isotopic composition of air trapped in ice cores. *Global Biogeochemical Cycles* 21: GB1025.

Landais A, Masson-Delmotte V, Combourieu Nebout N, et al. (2007b) Millennial scale variations of the isotopic composition of atmospheric oxygen over Marine Isotopic Stage 4. *Earth and Planetary Science Letters* 258: 101–113.

Lane GA and Dole M (1956) Fractionation of oxygen isotopes during respiration. *Science* 123: 574–575.

Laskar J, Robutel P, Joutel F, Gastineau M, Correia ACM, and Levrard B (2004) A long-term numerical solution for the insolation quantities of the Earth. *Astronomy and Astrophysics* 428: 261–285.

Levine NM, Bender ML, and Doney SC (2009) The $\delta^{18}O$ of dissolved O_2 as a tracer of mixing and respiration in the mesopelagic ocean. *Global Biogeochemical Cycles* 23: GB1006.

Luz B and Barkan E (2000) Assessment of oceanic productivity with the triple-isotope composition of dissolved oxygen. *Science* 288: 2028–2031.

Luz B and Barkan E (2005) The isotopic ratios $^{17}O/^{16}O$ and $^{18}O/^{16}O$ in molecular oxygen and their significance in biogeochemistry. *Geochimica et Cosmochimica Acta* 69: 1099–1110.

Luz B and Barkan E (2009) Net and gross production from oxygen/argon, $^{17}O/^{16}O$ and $^{18}O/^{16}O$ ratios. *Aquatic Microbial Ecology* 56: 133–145.

Luz B and Barkan E (2010) Variations of $^{17}O/^{16}O$ and $^{18}O/^{16}O$ in meteoric waters. *Geochimica et Cosmochimica Acta* 74: 6276–6286.

Luz B and Barkan E (2011) The isotopic composition of atmospheric oxygen. *Global Biogeochemical Cycles* 25: GB3001.

Luz B, Barkan E, Bender ML, Thiemens MH, and Boering KA (1999) Triple-isotope composition of atmospheric oxygen as a tracer of biosphere productivity. *Nature* 400: 547–550.

Luz B, Barkan E, Sagi Y, and Yacobi YZ (2002) Evaluation of community respiratory mechanisms with oxygen isotopes: A case study in Lake Kinneret. *Limnology and Oceanography* 47: 33–42.

Malaize B, Paillard D, Jouzel J, and Raynaud D (1999) The Dole effect over the last two glacial–interglacial cycles. *Journal of Geophysical Research* 104(D12): 14199–14208.

Marcus RA (2004) Mass-independent isotope effect in the earliest processed solids in the solar system: A possible chemical mechanism. *Journal of Chemical Physics* 121: 8201–8218.

Mason EA and Marrero TR (1970) The diffusion of atoms and molecules. *Advances in Atomic and Molecular Physics* 6: 155–232.

Masson V, Braconnot P, Jouzel J, de Noblet N, Cheddadi R, and Marchal O (2000) Simulation of intense monsoons under glacial conditions. *Geophysical Research Letters* 27: 1747–1750.

Matsuhisa Y, Goldsmith JR, and Clayton RN (1978) Mechanisms of hydrothermal crystallization of quartz at 250°C and 15 kbar. *Geochimica et Cosmochimica Acta* 42: 173–182.

Mauersberger K (1987) Ozone isotope measurements in the stratosphere. *Geophysical Research Letters* 14: 80–83.

Mehler AH (1951) Studies on reactions of illuminated chloroplasts. I. Mechanism of the reduction of oxygen and other Hill reagents. *Archives of Biochemistry and Biophysics* 33(1): 65–77.

Mélieres M-A, Rossignol-Strick M, and Malaizé B (1997) Relation between low latitude insolation and $\delta^{18}O$ change of atmospheric oxygen for the last 200 kyrs, as revealed by Mediterranean sapropels. *Geophysical Research Letters* 24: 1235–1238.

Miller MF (2002) Isotopic fractionation and the quantification of ^{17}O anomalies in the oxygen three-isotope system: An appraisal and geochemical significance. *Geochimica et Cosmochimica Acta* 66: 1881–1889.

Miller MF, Franchi IA, Thiemens MH, et al. (2002) Mass-independent fractionation of oxygen isotopes during thermal decomposition of carbonates. *Proceedings of the National Academy of Sciences of the United States of America* 99: 10988–10993.

Mills GA and Urey HC (1940) The kinetics of isotopic exchange between carbon dioxide, bicarbonate ion, carbonate ion and water. *Journal of the American Chemical Society* 62: 1019–1026.

Mook WG (ed.) (2000) *Environmental Isotopes in the Hydrological Cycle, vol. 1: Introduction*. Paris, Vienna: UNESCO/IAEA.

Morita N (1935) The increased density of air oxygen relative to water oxygen. *Journal of the Chemical Society* 56: 1291.

Prokopenko MG, Pauluis OM, Granger J, and Yeung LY (2011) Exact evaluation of gross photosynthetic production from the oxygen triple-isotope composition of O_2: Implications for the net-to-gross primary production ratios. *Geophysical Research Letters* 38: L14603.

Quay PD, Emerson S, Wilbur DO, Stump C, and Knox M (1993) The $\delta^{18}O$ of dissolved O_2 in the surface waters of the subarctic Pacific: A tracer of biological productivity. *Journal of Geophysical Research* 98(C5): 8447–8458.

Quay PD, Peacock C, Björkman K, and Karl DM (2010) Measuring primary production rates in the ocean: Enigmatic results between incubation and non-incubation methods at Station ALOHA. *Global Biogeochemical Cycles* 24: GB3014.

Quay PD, Wilbur DO, Richey JE, Devol AH, Benner R, and Forssberg BR (1995) The $^{18}O:^{16}O$ of dissolved oxygen in rivers and lakes in the Amazon Basin: Determining the ratio of respiration to photosynthesis rates in freshwaters. *Limnology and Oceanography* 40: 718–729.

Rabinowitch EI (1945) *Photosynthesis and Related Processes*, vol. 1. New York: Interscience.

Rakestraw NW, Rudd DP, and Dole M (1951) Isotopic composition of oxygen in air dissolved in Pacific Ocean water as a function of depth. *Journal of the American Chemical Society* 73: 2976.

Reuer MK, Barnett BA, Bender ML, Falkowski PG, and Hendricks MB (2007) New estimates of Southern Ocean biological production rates from O_2/Ar ratios and the triple isotope composition of O_2. *Deep Sea Research Part I: Oceanographic Research Papers* 54: 951–974.

Ribas-Carbo M, Berry JA, Yakir D, et al. (1995) Electron partitioning between the cytochrome and alternative pathways in plant mitochondria. *Plant Physiology* 109: 829–837.

Roughton FJW (1935) Recent work on carbon dioxide transport by the blood. *Physiological Reviews* 15: 241–296.

Sarma VVSS, Abe O, Yoshida N, and Saino T (2008) Spatial variations in time-integrated plankton metabolic rates in Sagami Bay using triple oxygen isotopes and O_2:Ar ratios. *Limnology and Oceanography* 53: 1776–1783.

Severinghaus JP, Beaudette R, Headly MA, Taylor K, and Brook EJ (2009) Oxygen-18 of O_2 records the impact of abrupt climate change on the terrestrial biosphere. *Science* 324: 1431–1434.

Severinghaus JP, Sowers T, Brook EJ, Alley RB, and Bender ML (1998) Timing of abrupt climate change at the end of the Younger Dryas period from thermally fractionated gases in polar ice. *Nature* 391: 141–146.

Sowers T, Bender M, and Raynaud D (1989) Elemental and isotopic composition of occluded O_2 and N_2 in polar ice. *Journal of Geophysical Research* 94: 5137–5150.

Thiemens MH (1999) Mass-independent isotope effects in planetary atmospheres and the early solar system. *Science* 283: 341–345.

Thiemens MH (2006) History and applications of mass-independent isotope effects. *Annual Review of Earth and Planetary Sciences* 34: 217–262.

Thiemens MH and Heidenrich JE (1983) The mass-independent fractionation of oxygen: A novel isotope effect and its possible cosmochemical implications. *Science* 219: 1073–1075.

Thiemens MH and Jackson T (1987) Production of isotopically heavy ozone by ultraviolet light photolysis of O_2. *Geophysical Research Letters* 14: 624–627.

Urey HC (1947) The thermodynamic properties of isotopic substances. *Journal of the Chemical Society* 1947: 562–581.

Urey CH and Greiff LJ (1935) Isotopic exchange equilibria. *Journal of the American Chemical Society* 57(2): 321–327.

Vinogradov AP, Kutyurin VM, and Zadorozhnyi IK (1959) Isotope fractionation of atmospheric oxygen. *Geokhimiya* 3: 195–207 (For English translation see *Geochemistry* 1959, 3: 241–253 (published by American Geological Institute)).

Waelbroeck C, Labeyrie L, Michel E, et al. (2002) Sea-level and deep water temperature changes derived from benthic foraminifera isotopic records. *Quaternary Science Reviews* 21(1–3): 295–305.

Wang X, Auler AS, Edwards RL, et al. (2007) Millennial-scale precipitation changes in southern Brazil over the past 90,000 years. *Geophysical Research Letters* 34: L23701.

Wang YJ, Cheng H, Edwards RL, et al. (2001) A high-resolution absolute-dated late Pleistocene monsoon record from Hulu Cave, China. *Science* 294: 2345.

Wang YJ, Cheng H, Edwards RL, et al. (2005) The Holocene Asian monsoon: Links to solar changes and North Atlantic climate. *Science* 308: 854–857.

Wang YJ, Cheng H, Edwards RL, et al. (2008) Millennial- and orbital-scale changes in the East Asian monsoon over the past 224,000 years. *Nature* 451: 1090–1093.

Welp L, Keeling RF, Meijer HAJ, et al. (2011) Interannual variability in the oxygen isotopes of atmospheric CO_2 driven by El Niño. *Nature* 477: 579–582.

West JB, Sobek A, and Ehleringer JR (2008) A simplified GIS approach to modeling global leaf water isoscapes. *PLoS One* 3(6): e2447.

Weston RE (1999) Anomalous or mass-independent isotope effects. *Chemical Reviews* 99: 2115–2136.

Yakir D, Berry JA, Giles L, and Osmond CB (1994) Isotopic heterogeneity of water in transpiring leaves: Identification of the component that controls the $\delta^{18}O$ of atmospheric O_2 and CO_2. *Plant, Cell and Environment* 17: 73–80.

Young ED, Galy A, and Nagahara H (2002) Kinetic and equilibrium mass-dependent isotope fractionation laws in nature and their geochemical and cosmochemical significance. *Geochimica et Cosmochimica Acta* 66: 1095–1104.

Yung YL, DeMore WB, and Pinto JP (1991) Isotopic exchange between carbon dioxide and ozone via $O(^1D)$ in the stratosphere. *Geophysical Research Letters* 18(1): 13–16.

Yung YL, Lee AY, Irion FW, DeMore WB, and Wen J (1997) Carbon dioxide in the atmosphere: Isotopic exchange with ozone and its use as a tracer in the middle atmosphere. *Journal of Geophysical Research* 102(D9): 10857–10866.